Title Page

Full title: Molecular characterization of nervous system organization in the hemichordate *Saccoglossus kowalevskii*

Short title: Nervous system organization in a hemichordate

Author List

José M. Andrade Lopéz, Ariel M. Pani, Mike Wu, John Gerhart, Christopher J. Lowe*

Author affiliation

1) Hopkins Marine Station, Department of Biology, Stanford University, 120 Oceanview Blvd., Pacific Grove, CA 93950, United States

2) Departments of Biology and Cell Biology, University of Virginia, 90 Geldard Drive, Charlottesville, VA 22903

3) Department of Molecular and Cell Biology, University of California, 142 Life Sciences Addition #3200, Berkeley, CA 94720-3200

* corresponding author

Abstract

Hemichordates are an important group for investigating the evolution of bilaterian nervous systems. As the closest chordate outgroup with a bilaterally symmetric adult body plan, hemichordates are particularly informative for exploring the origins of chordates. Despite the importance of hemichordate neuroanatomy for testing hypotheses on deuterostome and chordate evolution, adult hemichordate nervous systems have

not been comprehensively described using molecular techniques, and classic histological descriptions disagree on basic aspects of nervous system organization. A molecular description of hemichordate nervous system organization is important for both anatomical comparisons across phyla and for attempts to understand how conserved gene regulatory programs for ectodermal patterning relate to morphological evolution in deep time. Here, we describe the basic organization of the adult hemichordate *Saccoglossus kowalevskii* nervous system using immunofluorescence, *in situ* hybridization, and transgenic reporters to visualize neurons, neuropil, and key neuronal cell types. Consistent with previous descriptions, we found the *S. kowalevskii* nervous system consists of a pervasive nerve plexus that is concentrated in the anterior, along with nerve cords on both the dorsal and ventral sides. Neuronal cell types exhibited clear anteroposterior and dorsoventral regionalization in multiple areas of the body. We observed spatially demarcated expression patterns for many genes involved in synthesis or transport of neurotransmitters and neuropeptides but did not observe clear distinctions between putatively centralized and decentralized portions of the nervous system. In the trunk, there is a clear division of cell types between the dorsal and ventral cords suggesting differences in function. The plexus shows regionalized structure and is consistent with the proboscis base as a major site for information processing rather than the dorsal nerve cord. The absence of neural processes crossing the basement membrane into muscle and extensive axonal varicosities suggest that volumetric transmission may play an important role in neural function. These data now facilitate more informed neural comparisons between hemichordates and other groups and contribute to broader debates on the origins and evolution of bilaterian nervous systems.

Introduction

The evolution and origins of animal nervous systems has been a topic of debate in comparative literature for over a century, and the origins of the chordate nervous system has been a topic of particular interest (Bateson, 1886; Garstang, 1894; Garstang, 1928; Geoffroy-St. Hilaire, 1822). With the emergence of

molecular genetic data, the origins of brains and the deep ancestry of central nervous systems (CNS) has been a fascination in the field of evolution of development (Arendt and Nubler-Jung, 1996; De Robertis and Sasai, 1996; Denes et al., 2007; Hirth, 2010; Holland, 2015; Lowe et al., 2003; Martin-Duran et al., 2018). Classical comparative neurobiology has a rich and long history with broad phylogenetic sampling that was instrumental in developing many of the major hypotheses in neurobiology and nervous system evolution (Bullock and Horridge, 1965). The spectacular innovations in molecular neuroscience have given unprecedented insights into neural function (Luo, 2020). However, the focus of this work has been largely on biological models with highly centralized nervous systems and strong cephalization, particularly arthropods and vertebrates (Hejnol and Lowe, 2015). There have been fewer comprehensive molecular studies in phyla outside of these clades, particularly in animals with more sedentary lifestyles and less obvious centralization. Yet, for a broader understanding of nervous system evolution in metazoans, contemporary molecular data from these phyla is essential. This is now particularly pressing, as the generation of comparative developmental patterning data of regulatory genes, with key roles in CNS specification and patterning of arthropods and vertebrates, has now been investigated quite broadly phylogenetically, and by far outpaced parallel contemporary characterizations of neural cell type identity, and nervous system structure and function in the same representative species. Application of modern molecular tools of neurobiology to a wider range of species representing a broader sampling of neural systems is now essential, and not only test prevailing views on the evolution of the nervous system, but also provide novel opportunities to investigate neural circuit evolution.

Hemichordates are a group of marine invertebrates with sedentary adult life histories that have long been of comparative interest particularly in relation to chordate evolution (Kaul-Strehlow and Röttinger, 2015; Lowe, 2021; Tassia et al., 2016). Hemichordates were originally grouped within chordates due to proposed morphological affinities with chordates (Bateson, 1885). A close phylogenetic relationship with echinoderms based on larval morphology were recognized as early as the late 1800s (Metschnikoff, 1881), and all molecular studies have robustly grouped hemichordates as the sister group of echinoderms

within the deuterostomes (Bromham and Degnan, 1999; Cameron et al., 2000; Cannon et al., 2014; Furlong and Holland, 2002). Hemichordates are divided into two major lineages; Enteropneusta and Pterobranchia. Enteropneusta are free-living worms that mainly live in burrows feeding by filter feeding or by particle ingestion, whereas Pterobranchs are small, largely colonial animals that have received far less research attention, due to their scarcity and small size (Sato et al., 2008; Tassia et al., 2016).

The earliest descriptions of the nervous system of enteropneusts using classical staining methods began in the late 1800s (Bateson, 1886; Kowalevsky, 1866; Spengel, 1877, 1903) and continued sporadically in the early to mid 1900s (Bullock, 1940, 1944; Bullock, 1945; Dawydoff, 1948; Hess, 1937; Knight-Jones, 1952). Only a few studies have used electron microscopy for more detailed structural observations (Dilly, 1969; Dilly et al., 1970; Kaul and Stach, 2010; Kaul-Strehlow and Stach, 2013). The enteropneust nervous system is largely intraepidermal with a basiepithelial plexus throughout the animal, but more prominent anteriorly in the proboscis and collar, and thickest at the base of the proboscis and proboscis stem (Fig 1). There are two cords, one ventral that is basiepidermal, extending from the posterior collar to the posterior of the trunk, and dorsal cord that extends along the entire extent of the dorsal midline. From the anus to the collar, this dorsal cord is superficial and basiepidermal, but the cord is internalized in the collar into a subepidermal cord, which in some species resembles vertebrate neural tube (Bateson, 1886; Kaul and Stach, 2010; Luttrell et al., 2012). At its most anterior extent, the collar cord emerges at the proboscis stem and continues as a superficial cord along the length of the proboscis. The two cords are connected by a nerve ring in the posterior collar. Classical studies of hemichordate enteropneust nervous systems have come to contrasting conclusions on the most basic organizational principles of their structure and function. Some studies focused on the importance of the two cords, dorsal and ventral, acting as potential integration centers and concluded that hemichordates possess a CNS (Bateson, 1886; Hess, 1937; Morgan, 1894), whereas others have focused on the broadly distributed epithelial plexus with dorsal and ventral cords acting as conduction tracts instead of integration centers (Bullock, 1940; Bullock, 1945; Knight-Jones, 1952). From work in separate species, Bateson and Morgan concluded that the

enteropneust collar cord, an intraepidermal cord, was homologous to the dorsal cord of chordates (Bateson, 1886; Morgan, 1894) because of the striking similarities to the subepidermal hollow cord, that in some species forms by a morphological process that strongly resembles vertebrate neurulation. Later studies in the 1930s-50s hypothesize that the dorsal and ventral cord were conduction tracts that lack neural cell bodies (Bullock 1945, Knight-Jones 1952). Bullock believed that the hemichordate nervous system more closely resembled the nerve net of cnidarians (Bullock 1945) whereas Knight-Jones alternatively proposed that the collar cord may be homologous to the neural tube in chordates but had since been secondarily simplified and is now largely a through tract rather than an integrative center (Knight-Jones 1952). More recent studies based on comparative morphology have added support to the hypothesis of homology between the hemichordate collar cord and the chordate dorsal cord (Kaul and Stach, 2010; Luttrell et al., 2012)

Recent interest in bilaterian neural system evolution has been driven by body patterning comparisons and the remarkable similarities between the development of central nervous systems of distantly related nervous systems (Arendt and Nubler-Jung, 1994; De Robertis, 2008; De Robertis and Sasai, 1996; Hirth, 2010; Hirth and Reichert, 1999; Lichtneckert and Reichert, 2005). Most molecular insights into hemichordate neural development have been inferential, using patterning genes rather than genes with roles in neural cell type differentiation (Aronowicz and Lowe, 2006; Darras et al., 2018; Gonzalez et al., 2017; Lowe et al., 2006; Lowe et al., 2003; Pani et al., 2012; Yao et al., 2016). However, some studies have focused specifically on genes with established roles in neural specification and differentiation, or cross-reactive antibodies for neural epitopes (Cunningham and Casey, 2014; Kaul-Strehlow et al., 2015; Lowe et al., 2003; Miyamoto et al., 2010; Nomaksteinsky et al., 2009). These studies have used pan-neural markers, like *elav* and synaptotagmin, and enzymes involved in neurotransmitter synthesis to study the hemichordate nervous system. Although limited, these studies have continued to show evidence of a broad plexus, but again have come to contrasting conclusions about the nature of the enteropneust nervous system. There is still no comprehensive study of neural subtypes and their distribution in

hemichordates, nor a clear picture of the morphology for different cell types or structure of the neural plexus and cords.

Speculation on the organization of the enteropneust nervous system was reignited with the studies on the expression of gene regulatory networks (GRN) with conserved roles in patterning the CNS of many model species during the early development of *S. kowalevskii*. The GRN for anterior-posterior CNS patterning that is well conserved between several protostomes groups and chordates is also conserved in hemichordates along the anterior-posterior (AP) axis even though the nervous systems they specify are anatomically very different (Darras et al., 2018; Gonzalez et al., 2017; Kaul-Strehlow et al., 2017; Lowe et al., 2003; Pani et al., 2012; Yao et al., 2016). These genes are expressed in circular bands around the ectoderm in hemichordates, rather than expressed in a tight domain associated with either the dorsal or ventral cords, unlike in vertebrates where they are most prominently expressed in the developing brain and nerve cord (Pani et al., 2012). The neural structures specified by this conserved network have evolved independently and represent highly divergent structures despite the tight conservation in their gene regulatory networks. Therefore, it remains an open question as to whether there are some elements of neural conservation despite the overt differences in the organizational elements of their respective nervous systems. It also remains a possibility that there are neural cell type homologies under conserved positional regulation between vertebrates and hemichordates. A closer examination of the molecular neurobiology of hemichordates and the potential link to conserved suites of regulatory genes will contribute to the discussion about how molecular genetic data can be used to reconstruct ancestral neural architectures.

Here we characterize the expression of multiple neural markers using *in situ* hybridization, and immunohistochemistry to characterize the location and degree of specialization of the nervous system along both the AP and dorsal-ventral (DV) axes, and the extent and structure of the neural plexus. We also used mosaic transgenic approaches to determine cellular morphologies and projection patterns of

neural subpopulations. Our data provides the first comprehensive description, to our knowledge, of an adult hemichordate nervous system using molecular methods, which will facilitate comparisons to other bilaterians.

Results

Extent and regionalization of neural markers along the A/P and D/V axes

Many classical studies of enteropneust nervous systems used histological techniques, such as Golgi stains, that generally work well in animals with a clearly defined CNS where neurons are segregated from the general epithelium. However, these methods may not unambiguously distinguish neural from epidermal cells in animals, like enteropneusts, where the nervous system is intraepidermal. Consequently, the number, diversity, and distribution of neurons along the A/P and D/V axes of the adult animals has been a source of controversy (Bullock, 1945). We examined expression of a wide range of neural/neurosecretory markers in post-hatching juvenile and fully grown adult animals, using *in situ* hybridization. Previous studies have demonstrated that neurons are specified across broad domains during embryogenesis, and nerve cords are first apparent during late stages of embryonic development (Cunningham and Casey, 2014; Kaul-Strehlow et al., 2015). Our study focused on post-hatching juveniles as the animal possesses almost all the adult characteristics but are smaller and more amenable to whole-mount microscopy. This initial part of our study establishes a more accurate assessment of neural cell body number, the extent of neural subtypes, and how they are distributed along the major organizational axes.

***Elav* expression in the *S. kowalevskii* nervous system:** *Embryonic lethal abnormal visual system (elav)* is a conserved RNA binding protein, first discovered in *Drosophila melanogaster* that has been used in

174 many organisms as a putative pan-neuronal marker (Cunningham and Casey, 2014; Robinow et al., 1988;
175 Robinow and White, 1988). However, expression of *elav* has been reported in other cell types, and does
176 not always mark the entire neural complement (Pham and Hobert, 2019; Sanfilippo et al., 2016), so
177 caution should be used when only using this marker to fully represent neural complements in developing
178 models. We first sought to identify the distribution of *elav*+ cells in juveniles and adult tissue by *in situ*
179 hybridization, extending the scope of previous studies at earlier developmental stages (Cunningham and
180 Casey, 2014; Lowe et al., 2003). This gene has previously been shown to exhibit a tight association with
181 the forming cords on the trunk midlines and expressed broadly in the proboscis ectoderm (Cunningham
182 and Casey, 2014; Lowe et al., 2003; Nomaksteinsky et al., 2009), but with few cells outside of the cords,
183 posterior to the collar.
184
185 We first examined *elav* expression in adult *S. kowalevskii* through a comprehensive series of adult
186 sections in both transverse and sagittal planes (Fig 1A). The transverse plane at mid-proboscis shows
187 circumferential *elav* expression in the most basal layer of the epithelium, and more marked staining along
188 the dorsal midline (Fig 1B). The cross section at the proboscis base has a thicker band of expression,
189 supporting previous observations of neural condensation in this region (Nomaksteinsky et al., 2009) (Fig
190 1C). At the anterior collar, we detected expression of *elav* throughout the pharyngeal epithelium (Fig 1D-
191 G) and evidence of the anterior collar nerve ring in the ectoderm (Fig 1D). In addition, there is a
192 prominent layer of *elav* expression dorsal to processes in the dorsal cord, representing the soma of that
193 runs the length of the collar as an internal collar cord (Fig 1D-I). Expression in the general ectoderm of
194 collar and trunk is sparse, as described previously in *Ptychodera flava* (Nomaksteinsky et al., 2009) but
195 cells are detected in the epithelium in the posterior collar and trunk (Fig 1H-J). Sagittal sections show a
196 gradient of *elav* expression in the proboscis increasing towards the base, an anterior collar ring (ACR) and
197 posterior collar ring, and expression in the pharyngeal endoderm (Fig 1K,L,M). The middle sagittal
198 section clearly shows the trajectory of the collar cord (Fig 1L). The enteric nervous system is also visible
199 in the endoderm with dispersed *elav*+ cells in the gut (Fig 1M). At late juvenile stage, characterized by

the presence of 3-gill slits (3GS), *elav*+ cells are distributed similarly to their distribution in adults; throughout the proboscis ectoderm, with a concentration at the proboscis base, and also along the entire dorsal and ventral cords (Fig 1N). The proboscis dorsal cord is also visible and extends anteriorly from the collar cord (Fig 1O). The similarities between adult and late juvenile suggests that the juvenile is a reasonable approximation for basic organization of adult neural characters.

Given the comparative interest in hemichordate trunk nerve cords and distribution of neurons in the skin, we examined *elav* expression closely in adults using whole mount *in situ* hybridization to visualize cell populations that may be difficult to observe in tissue sections. In the ventral cord, expression of *elav* is broadly expressed in a wide band of ectoderm. Rows of clustered cells are present in columns, perpendicular to the cord, along ridges of the epithelium (Fig 1P). On the dorsal side, a thin line of *elav*+ cells is present along the length of the proboscis (Fig 1Q), along with the broad expression shown in sections (Fig 1B,C). Expression is also detected in two narrow rows of cells that flank the dorsal midline along the length of the trunk (Fig 1R,S). In the trunk, the *elav*+ domain is markedly narrower on the dorsal side than the ventral side. In the posterior trunk, *elav*+ cells are also distributed in clusters of cells throughout the epithelium, possibly associated with the calcified granules embedded in this region (Fig 1S).

Regionalization of neural subtypes

Expression of neurotransmitter and neuropeptide biosynthesis and transport markers: While general neural markers like *elav* give a broad picture of the localization of neurons, they do not give any insights into the extent of neural diversity, or how neural subpopulations are organized. Expression of genes involved in the biosynthesis and transport of neurotransmitters and neuropeptides provides information about the extent of neural differentiation, and how organized their expression domains are

along organizational axes. We performed *in situ* hybridization for components of neurotransmitter and neuropeptide signaling, including proteins involved in their synthesis and transport in juvenile, both at the 1 gill-slit (1GS) and 3GS stage, and in some cases, in adult tissue.

Neurotransmitters are small molecules used by neurons as chemical messengers to communicate across cells. They can transmit an excitatory or inhibitory signal synaptically, or modulate neuronal activity non-synaptically using biogenic amines (or monoamines) and amino acids. Genes involved in neurotransmitter synthesis and transport are often highly regionalized in the nervous systems of model bilaterian species.

Monoamine neurotransmitters: In *Saccoglossus* juveniles, the location of catecholaminergic neurons is revealed by the expression of *tyrosine hydroxylase* (*TH*) in scattered cells at several different domains in the ectoderm. Early developmental stages were examined previously (Cunningham and Casey, 2014). In early juveniles, shortly after hatching *TH* expression is restricted to isolated cells in the anterior proboscis ectoderm, and broadly in the anterior trunk, wrapping around the forming first gill slit (Cunningham and Casey, 2014; Pani et al., 2012). This pattern continues in the later juvenile stages before hatching with the addition of a thin circumferential line close to the base of the proboscis (Fig 2A). The expression around the gill slits is far more diffuse and extensive than the more cell type specific staining in the proboscis and collar (Fig 2A,A',C). In post hatching juveniles, an additional prominent band of cells forms at the anterior tip of the collar (Fig 2A'). The same general expression domains persist through to adults, but with an expanded anterior proboscis domain (Fig 2B), and additional isolated cells in the collar, with a strong anterior collar domain, and row of cells at the base of the proboscis (Fig 2B'). To specifically identify dopaminergic neurons, we examined the expression of *dopamine transporter* (*DAT*). In juveniles, *DAT* is co-expressed in many of the same cells in the juveniles (Fig 2C); in the anterior proboscis (Fig 2C') and in anterior collar (Fig 2C''). *TH*+ cells at the base of the proboscis were conspicuously missing *DAT* co-expression, raising the possibility they may represent other types of catecholaminergic neurons.

However, in older juveniles, *DAT* is expressed in this region and supports the DA neural identity (Fig 2C'''').

The distribution of *tryptophan hydroxylase* (*TPH*), marking serotonergic neurons, was previously reported at earlier developmental stages (Cunningham and Casey, 2014). Here we confirm isolated cellular expression in a broad circumferential domain in the proboscis ectoderm shortly after hatching (Fig 2D). Histamine is synthesized from histidine by *histidine decarboxylase* (*HDC*) and is a marker for histaminergic neurons (Watanabe et al., 1984). In juveniles, expression of *HDC* is sharply defined in the posterior proboscis in a broad ectodermal domain rather than punctate individual cells, which may indicate a broader ectodermal distribution of histamine rather than specifically neuronal (Fig 2E). Additionally, more punctate staining is detected in the ventral ectoderm narrowing to the ventral cord at later stages, and scattered large cells along the dorsal cord in the trunk, which refine to a more posterior territory at later stages (Fig 2E,E').

Amino acid neurotransmitters: Two major amino acid neurotransmitters are glutamate and GABA. Glutamate is a major excitatory neurotransmitter across bilaterians and non-bilaterians (Antzoulatos and Byrne, 2004; Danbolt, 2001; Fonnum, 1984; Greer et al., 2017; Nistri and Constanti, 1979). GABA has a conserved role in bilaterians as an inhibitory neurotransmitter in both the CNS and PNS in invertebrates and vertebrates (Gerschenfeld, 1973; Jackson et al., 1990; McIntire et al., 1993; Miller, 2019; Mueller et al., 2006; Nistri and Constanti, 1979; Roberts et al., 1976). Expression of *glutamate decarboxylase* (*GAD*) has been used to characterize the distribution of GABA–producing neurons (Roberts and Kuriyama, 1968) along with the GABA transporter *VGAT* (Kinjo et al., 2013), whereas glutamatergic neurons have been identified by the expression of its transporter, *VGluT*.

In *Saccoglossus* juveniles, *VGluT* is detected in isolated cells in the ectoderm of the proboscis and anterior collar (Fig 2F). In the trunk, it is detected in two rows of cells on either side of the dorsal midline

along the trunk, posterior to the collar (Fig 2F, inset) at early juvenile stage and in scattered cells broadly in the posterior. In 3GS juveniles, expression in the proboscis remains broadly dispersed, and there are two circumferential lines of cells in both the anterior and posterior collar (Fig 2F'). Expression extends down the trunk, again along the dorsal midline in a broad territory, wider than the extent of the cord defined by the expression of *elav* (Fig1N,O,R), but also dispersed in the general ectoderm (Fig 2F''). *GAD* is expressed in scattered ectodermal cells in defined domains throughout different developmental stages. In early juveniles it is expressed throughout the entire proboscis, but most prominently in the anterior tip and at the proboscis base (Fig 2G). At later juvenile stages, the anterior and posterior ectodermal, circumferential domains become more prominent, and a sharp, narrow band of expression at the very anterior lip of the collar is detected in a circumferential domain. At these later stages, expression is now detected in isolated cells in the posterior region of the pharynx and in scattered cells in the dorsal cord of the trunk (Fig 2G'). The juvenile expression is consistent with the patterns found in adult animals: the whole mount *in situ* hybridization of adult *GAD* expression reveals a dense anterior expression domain that becomes increasingly diffuse down towards the proboscis base (Fig 2H). There is a pronounced ring of cells at the proboscis base that is contiguous except dorsally where the ring terminates with a pair of prominent cell clusters on either side of the dorsal midline (Fig 2H'). The anterior lip of the collar has a similar ring in isolated cells (Fig 2H'). The distribution of the GABA transporter *VGAT* in early juveniles shows very similar expression domains to *GAD* at early juvenile stages, with strong expression at the base of the proboscis and cells scattered throughout the ectoderm (Fig 2I,I'). However, we do not observe expression in the anterior proboscis where *GAD* is localized at either early or late juvenile stage.

Neuropeptides: Neuropeptides are the largest and most diverse signaling molecules ranging from 3-40+ amino acids that are involved in neurotransmission, neuromodulation or hormonal functions (Burbach, 2011; van den Pol, 2012). Most neuropeptides signal through G protein-coupled receptors (GPCRs) to

modulate downstream activities (Hewes and Taghert, 2001; Jekely, 2013). Previous studies have identified an array of conserved neuropeptides and their GPCR receptors in *S. kowalevskii* (Elphick, 2010; Elphick and Mirabeau, 2014; Jekely, 2013; Krishnan et al., 2013; Mirabeau and Joly, 2013). Three general neuropeptide synthesis enzymes are Prohormone convertase 2 (PC2), glutaminyl-peptide cyclotransferase (GPC), and peptidyl glycine α-amidating monooxygenase (PAM), which catalyzes the posttranslational modification of the N-terminal glutamine (GPC) or the C-terminal glycine (PAM) of peptide hormones (Busby et al., 1987; Fischer and Spiess, 1987; Rouille et al., 1995; Seidah et al., 1999; Zhang et al., 2010). Expression of these markers reveals the general regional expression of the diverse array of neuropeptides in *S. kowalevskii.* Expression of these enzymes exhibit generally overlapping localization in both early and late juveniles (Fig 3A-B), with many cells co-expressing multiple neuropeptide synthesis markers (Fig 3C-C'''). In early juveniles, PC2 is broadly expressed in the proboscis, but strongest at the base (Fig 3D). It has a tight ring of expression in the anterior collar, in the collar/dorsal cord, and in the developing ventral cord (Fig 3D). Expression in the later juvenile is strongest at the base of the proboscis, anterior collar ring, and anterior ventral cord, whereas expression in the anterior proboscis and dorsal cord becomes less prominent (Fig 3D'). GPC expression is more dorsally localized at the proboscis base with more punctate expression in the ventral ectoderm (Fig 3E,E') whereas PC2 expression is more uniform in a thick band around at the proboscis base (Fig 3D,D'). We also observed expression in the more posterior regions of the dorsal and ventral cords. Together, these enzymes are expressed at the five major regions of the ectoderm: anterior proboscis, posterior proboscis, anterior collar, dorsal cord, and the ventral cord and overlap in their expression domains in the proboscis and collar with several of the neurotransmitter systems.

A wide range of neuropeptides have been identified in *S. kowalevskii* (Elphick, 2010; Elphick and Mirabeau, 2014; Jekely, 2013; Krishnan et al., 2013; Mirabeau and Joly, 2013), and we investigated the expression of a small subset of these. A major group of diverse neuropeptides have a typical c-terminal

signature, many of which are phyla-specific, including the RFamides, which have the conserved c-terminal RFamide amino acid sequence. There are hundreds of RFamides that have been described across bilaterians, and each is involved in diverse roles ranging from osmoregulation, muscle contractions, reproduction, feeding and digestion (Elphick and Mirabeau, 2014; Jekely, 2013; Mirabeau and Joly, 2013; Walker et al., 2009). The original RFamide, FRMRamide, was identified from the ganglia of a mollusk, *Macrocallista nimbosa*, and was later characterized for its role as a caridioexcitatory neuropeptide (Price & Greenberg 1977).

S. kowalevskii contains many of these neuropeptides with a signature c-terminal sequence including VIamide, Luqin (RWamide), WFMRFamide, and NNFamide. VIamide is characterized by an anterior, dorsal domain of expression in early and late juveniles, with isolated cells along the dorsal midline from the anterior tip to about half way down the proboscis (Fig 3G,G'). The conserved bilaterian neuropeptide luqin (Luq), subsequently lost in the chordate lineage (Elphick and Mirabeau, 2014), is an RFamide-related neuropeptide. Comparative studies across bilaterians suggest a shared role in chemosensory and locomotion control through flask shaped, ciliated RFamide neurons (Tessmar-Raible et al., 2007). Luq is initially expressed in the posterior proboscis and anterior collar at the 1GS stage but expression is later detected at the anterior and posterior proboscis, anterior collar, both the dorsal and ventral cord, and the ventral cord extends towards the post anal tail in 3GS juveniles (Fig 3H,H'). WFMRFamide expression appears as scattered cells in the anterior proboscis and strong circular bands at the proboscis base and anterior collar in both early and late juveniles (Fig 3J,J'). Expression also appears in the trunk around the gill slits and ciliary band in late juveniles (Fig 3J'). NNFamide is expressed in the proboscis ectoderm in two main domains; the most prominent is in a strong, circumferential, horseshoe-shaped band with expression absent in the most dorsal territory, close to the base of the proboscis (Fig 3K,K'). The second domain is defined by scattered individual cells visible in the entire anterior half of the proboscis ectoderm, all the way to the anterior tip.

The hypothalamic-pituitary axis (HPA) is a major neuroendocrine system associated with the regulation of many biological and physiological mechanisms including regulating metabolism, immune system, stress, reproduction, growth, and development by acting on endocrine glands like the adrenal, gonads, and thyroid (Lechan & Toni 2016, Rosol et al 2001, Kanda 2019, Zoeller et al 2007). Neurons from the hypothalamus regulate the pituitary and downstream organs including the gonads, adrenal gland, and thalamus by stimulating the release of neuropeptides conserved across bilaterians (Jékely 2013, Mirabeau & Joly 2013, Bauknecht & Jékely 2015, Elphick & Mirabeau 2014, 2018). The *S. kowalevskii* genome contains many of these conserved neuropeptides including vasotocin, orexin, gonadotropin-releasing hormone (GnRH), corticotropin-releasing hormone (CRH), thyrotropin-releasing hormone (TRH), and calcitonin (CalC), which have all been identified in previous studies (Mirabeau & Joly 2013, Jékely 2013, Tian et al 2016, Semmens et al 2016). Vasotocin and orexin are two bilaterian-conserved neuropeptides secreted in the hypothalamus in vertebrates. Vasotocin is expressed in scattered cells at the trunk in early and late juveniles (Fig 3F,F'), whereas orexin is broadly expressed throughout the epithelium in early and late juveniles, with minimal expression around the collar (Fig 3M,M'). GnRH stimulates secretion of gonadotropins from pituitary neurons to regulate gametogenesis and gonadal development in both vertebrates (Kawada et al 2013, Sakai et al 2017). In *S. kowalevskii*, GnRH neurons are located in scattered cells at the proboscis base and in a similar domain to vasotocin at the trunk in early juveniles (Fig 3I). Neurons in the trunk have a visible proximal projection into the plexus, shown in the in the inset image (Fig 3I). Late juveniles have a strong ventral cord expression, with few cells along the dorsal cord and dorsal proboscis base (Fig 3I'). Inset image shows the dorsal view with expression at the dorsal proboscis base and along the dorsal cord in a late juvenile (Fig 3I'). CRH neurons in the vertebrate hypothalamus signal to the anterior pituitary and stimulating the release of adrenocorticotropic hormone into the bloodstream to regulate the stress response (Brunson et al 2013, Lovejoy et al 2014). CRH is expressed throughout the proboscis in early juveniles (Fig 3L) and becomes restricted to the heart-kidney complex overlying the stomocord and dorsal vessel, and along the dorsal cord in late juveniles (Fig 3L').

CalC and TRH are two additional HPA neuropeptides associated with thyroid function. CalC helps control plasma calcium levels to regulate bone remodeling and metabolism in vertebrates (Zoeller et al 2007, Carter & Schipani 2006, Naot & Cornish 2008) and is thought to have an ancestral role in regulating biomineralization (Cardoso et al 2020). CalC expression is seen in the posterior part of the proboscis in scattered cells in both early and late juveniles (Fig 3N,N') and along the ventral cord in late juveniles (Fig 3N'). Inset panel in Figure 3N show posterior projections of these neurons. TRH is expressed in scattered cells in the anterior proboscis, strong expression in the dorsal proboscis base, and along the trunk in early juveniles (Fig 3O). Cells at the trunk become restricted to the ventral cord in late juveniles (Fig 3O'). In both early and late juveniles, there are two dominant cell clusters adjacent to the dorsal proboscis base.

Other conserved neuropeptides within bilaterians include achatin and cholecystokinin (Elphick and Mirabeau, 2014; Elphick et al., 2018; Jekely, 2013). Achatin shows restricted expression in large isolated cells distributed in the anterior proboscis (Fig 3P,P'). Cholecystokinin (CCK) is a gastrointestinal hormone peptide that has an ancient role in regulating feeding (Tinoco et al., 2021). CCK is expressed in the proboscis base in early juveniles (Fig 3Q) and later has broader expression in the pharynx endoderm and ventral trunk ectoderm in late juveniles (Fig 3Q').

Many of the neuropeptides show dense expression at the base of the proboscis so we tested whether there was coexpression of multiple peptides, or each neural subtype associated with specific neuro peptides. We performed multiplexed HCR for three peptides, NNFamide, TRH, and WFMRFamide (Fig 3R-R'''), all expressed in similar domains. The anterior proboscis shows non-overlapping expression of the three markers evenly distributed across the epithelium across both stages (Fig 3R,R''), and the posterior proboscis is composed of non-overlapping rings of expression of individual neuropeptides (Fig 3R',R'''). The minimal neuropeptide coexpression suggests that neuropeptides may be good markers for specific neural cell types in the proboscis.

Unlike neurotransmitters, which preferentially exhibit anterior expression, neuropeptides show more extensive posterior expression along the ventral and dorsal cords. Expression data for neurotransmitter and neuropeptide synthesis and transport markers suggests that *S. kowalevskii* has a strongly regionalized nervous system, with an increased neural cell type diversity in 5 main territories; the anterior proboscis, posterior proboscis, anterior collar, dorsal cord, ventral cord; but most prominently, the dorsal proboscis base.

Plexus and neural cord organization

In the previous section we described the expression of many important genes involved in neural function by *in situ* hybridization. These data provide useful information about specialization and location of neuronal cell bodies, but tells us little about neural morphology, neurite and axonal projections, and the general structure of the nervous system. To begin to investigate nervous system structure and function, we performed immunohistochemistry for a monoclonal antibody (1E11) to the pan-neural marker synaptotagmin, which was developed from the radial nerve extract of asteroid, *Asterina pectinifera* (Nakajima et al., 2004b), to visualize cell morphology and neurite projections in juveniles and adults (Fig 4A). Previous comparative work has validated the cross reactivity of this antibody localizing to neurons in other ambulacrarian taxa; broadly in echinoderms and in another species of hemichordate (Byrne et al., 2007; Nakajima et al., 2004a).

Whole mount immunohistochemistry of late juveniles at the 3GS stage revealed a complex and structured nervous system with a dense basiepithelial nerve plexus throughout the proboscis, but thicker at the base (Fig 4A). Neurites and axons are well-labelled, but cell bodies had weak signal (Fig 4B). The plexus is also very prominent in the collar ectoderm, but much less in the trunk. An endodermal plexus is visible throughout the pharynx. The subepidermal collar cord is clearly visible extending from the thick plexus at

the dorsal posterior ectoderm of the proboscis into the superficial dorsal cord, which begins in the posterior collar and runs the length of the trunk terminating at the anus. The wider superficial ventral cord begins at the posterior collar/anterior trunk boundary and extends posteriorly throughout the entire ventral midline of the animal.

We further utilized 1E11 to determine the structure of the nervous system in adults. As many of the neural cell type markers exhibit localized domains of expression in the proboscis, we first investigated 1E11 expression at this site. We examined the plexus in this territory by peeling off sections of ectoderm from the underlying proboscis mesoderm in fixed adults and carrying out whole mount immunohistochemistry on these tissue fragments (Fig 4C). In the general proboscis ectoderm, we observe a well-organized plexus with parallel bundles of processes running along the AP axis, with regularly spaced connectors projecting laterally between the bundles (Fig 4D). This organization is remarkably similar to the drawings of Knight-Jones (1952). The dorsal superficial cord is visible as a thickening of this plexus (Fig 4E). The neurite bundles projecting along the AP axis observed in the mid proboscis exhibit a striking transition in plexus structure: a complex architecture of thicker neurite bundles forming a series of layered, interconnected tracks. This can be clearly observed in Figure 4D where the flat mount of the ectoderm shows the parallel projections on the left of the panel projecting into the complex plexus at the proboscis base at the right of the panel. A z-stack of this territory more clearly shows the structure of the plexus (Supplementary Movie 1). Higher magnification shows the complex architecture of this territory (Fig 4F,G). The structure of this domain is very reminiscent of the anterior territory of the plexus structure in the acoel *Hofstenia miamia* (Hulett et al., 2020) and the holes in the plexus may represent extensions from epithelial cells that attach to the basement membrane as reported from early EM studies (Dilly, 1969). Moving posteriorly into the collar, we observed a similar, structured plexus to the proboscis base, but with less densely packed tracts (Fig 4H). A z-stack (Supplemental Movie 2) in this region again clearly shows the structured nature of this plexus. Further posterior in the trunk, the plexus is less extensive than

453 in the proboscis or collar, with the dorsal and ventral cords being the most prominent features
454 representing condensations of the plexus along both midlines (Fig 4I).
455
456 The results from 1E11 reveal many general aspects of the distribution and organization of the neural
457 plexus, but little resolution of individual neurites. We used injection of lipophilic dye (DiI) into adult
458 fixed tissue in the mid proboscis to look more closely at the morphology and directionality of neurite
459 projections. Individual neurites extend from the injection site in all directions, but with prominent neurite
460 bundles projecting along an AP axis, matching what was observed with the IE11 antibody (Fig 4J,K). The
461 plexus is clearly structured, with the imaging stacks showing different projection patterns according to the
462 position along the apico/basal axis in the plexus. Lower volume injections of DiI imaged at higher
463 magnification reveal many neurites with regular puncta along their length (Fig 4L,M). As these swellings
464 may represent fixation artifacts, we utilized a live neural stain, NeuO, a membrane-permeable fluorescent
465 probe (Er et al., 2015). We observe similarly labeled neurites/axons in the trunk revealing regularly
466 spaced boutons along the neurites/axons (Fig 4N). The similar structures detected along the processes
467 using both fixed (DiI) and live (NeuO) tissue suggest these structures may represent either *en passant*
468 synapses (de Castro, 1950), or varicosities involved in volumetric release (Nieuwenhuys, 2000).
469

470 **Morphology and projection of neural subtypes**

471 Our *in situ* hybridization data for neurotransmitter and neuropeptide synthesis and transport markers
472 clearly demonstrates that *S. kowalevskii* has strong regional specialization of its nervous system, and also
473 revealed the location of cell bodies characterized by specific neurotransmitters and neuropeptides.
474 However, these data provide no information about the directionality or length of projections, and *in situ*
475 hybridization data rarely provides information about cellular morphology. We used two different methods
476 to investigate details of neural subtype morphology and projections; cross reactive antisera to
477 neurotransmitters and neural transgenics.

478

479 **Cross reactive antisera**

480 **Serotonergic neurons**: We used an antibody raised to 5-HT to label serotonergic neurons in 3GS stage *S.*
481 *kowalevskii* (Fig 5A). Previous work using this antibody has already investigated the distribution of the
482 serotonergic nervous system in early developmental stages, in juveniles and limited sections in adults, and
483 our data confirms expression and extends sampling of these studies (Brown et al., 2008; Cunningham and
484 Casey, 2014; Kaul-Strehlow et al., 2015). Figure 5 shows the distribution of the serotonergic nervous
485 system in juveniles and adults. In juveniles, the serotonergic nervous system is composed of primarily
486 receptor, flask-shaped bipolar neurons broadly dispersed in the proboscis ectoderm and collar, but more
487 sparsely in the trunk. In the proboscis, while staining is broadly scattered, there are no cell bodies detected
488 in either the most apical ectoderm or at the base of the proboscis (Fig 5A,C). All neurons project into the
489 underlying neural plexus, although it is not possible to trace the full length of individual axons due to
490 large numbers of projections in the plexus. However, proboscis neurons appear to generally project
491 posteriorly, based on the orientation of the axon close to the cell body. In the collar, cell bodies are
492 organized into three rings, two at the anterior and one at the mid collar (Fig 5A,D). These neurons also
493 have a single dendrite and sensory cilium projecting out of the epithelium, and a single axon projecting
494 basally into the neural plexus. There are positional differences in cell body location within the epithelium;
495 some cell bodies are located basally and others more apically (Fig 5B). In the collar and proboscis, we see
496 no dorsoventral differences in the distribution of cell bodies, however, cell bodies in the trunk are
497 positioned on the dorsal side, mostly lateral to the dorsal cord but generally project ventrally into the
498 ventral cord (Fig 5E). In the anterior part of the trunk, there are also cell bodies scattered in the ectoderm
499 more laterally around the gill slits (Fig 5A). A z-stack of the serotonergic nervous system in this region
500 again clearly shows the structured nature of this plexus, as well as dorsal sensory cells projecting laterally
501 along the trunk towards the ventral cord (Supplementary Movie 2).

502

We further extended our analysis into adult animals. Whole mount immunohistochemistry in adults show a far more extensive serotonergic population than in juveniles but generally confirm a similar expression pattern established in juveniles. Figure 5F shows a view of the mid-proboscis, showing broad distribution cell bodies projecting into the underlying epithelium, with projections in all directions, but most projecting posteriorly, similar to the organization revealed from 1E11 (Fig 4E). The base of the proboscis (the same specimen as Fig 4D,E) double labelled for both 1E11 and 5HT (Fig 5G,H) reveals that serotonergic axons form a subset of the complex network of bundles. The morphology of the neurites shows swellings along the length of the processes similar to what we demonstrated with DiI labelling. In the collar (Fig 5I), staining is absent in the anterior lip, but just posterior there is a ring of expression in the ectoderm, and broad ectodermal labelling throughout the collar ectoderm. Cell bodies are more broadly dispersed throughout the collar epithelium, rather than in discrete rings as in 3GS juveniles. Note that these findings contrast with the lack of neural staining from *elav* in this region (Fig 1). In the posterior trunk, the epithelium is ruffled, and we observed patches of cell bodies in the lateral body wall, and an extensive, but thin, plexus throughout the trunk epithelium (Fig 5J).

We next investigated the labelling of the serotonergic neurons in representative cross sections along the adult body, counterstained with phalloidin (Fig 5K). In the posterior proboscis, we observe clear dorsoventral asymmetry in plexus thickness, with the dorsal region thicker than the ventral territory, and with cell bodies distributed more ventrally in this plane of section (Fig 5L). In the mid-collar (Fig 5M) the neural plexus is extensive in both the ectoderm and the endoderm but is thinner than the proboscis plexus (Fig 5L). The dorsal cord is clearly visible and shown in higher magnification in Fig 5N: DAPI labels the soma of the cord positioned above the neurites that project through the cord, and as reported elsewhere, there is no obvious cord lumen. We did not observe any 5HT+ cell bodies in the cord soma in the limited sections we examined. As observed in the whole mount (Fig 5M), there is a broad distribution of cell bodies projecting into the plexus, without any dorsoventral differences. The pharyngeal epithelium also shows a prominent plexus throughout the pharynx, yet only a few isolated cell bodies are associated with

the endoderm in these sections. Sections in the anterior trunk show cell bodies sparsely scattered throughout the ectoderm with a thin ectodermal plexus that thickens ventrally, and the dorsal cord showing far fewer axons labelled than in the ventral cord. The endodermal plexus is very sparse (Fig 5O). In the posterior trunk, labelling of axons in the ventral cord is more prominent and a thin plexus is detected throughout the epithelium with scattered, isolated cell bodies (Fig 5P,Q). No endodermal plexus was detected.

GABAergic neurons: We used a GABA polyclonal antibody to stain GABAergic neurons in juveniles, as has been previously demonstrated in another enteropneust species, *P. flava* (Nomaksteinsky et al., 2009). To address concerns about antibody binding specificity, we compared GABA antisera reactivity with the *in situ* hybridization for GAD (Fig 2). We observed good concordance between the antibody and *in situ* hybridization localizations. The GABAergic nervous system in juveniles is concentrated both in the anterior and posterior proboscis ectoderm (Fig 6A,Ai). In the collar, there are two ectodermal rings of cells at the lip of the collar (Fig 6A). In the trunk, there are isolated neurons along the dorsal midline in both the ectoderm and endoderm (Fig 6Aii). These cells appear similar in morphology to 5HT+ cells; bipolar with a single neurite extending from the cell body to the apical region terminating with an apical cilium, and the axon descending into the plexus on the basal side. There are also dorsal endodermal neurons with a neurite projecting to the apical surface of the endoderm, but with the cell body embedded in the endodermal plexus (Fig 6Aii). Further posteriorly, there are prominent axonal projections around the gill slits and into the ventral cord (Fig 56iii).

The number of cell bodies at the proboscis, collar, and trunk increases substantially in adults. The base of the proboscis forms a similar pattern of GABA+ neurite bundles to those detected from 1E11 and 5HT (Fig 6B). The adult collar has a more expansive concentration of neurons with the anterior ring and scattered cell bodies throughout the collar ectoderm (Fig 6C). GABAergic neurons are labeled in gill bars (Fig 6D) with cell bodies projecting axons ventrally. To directly image the dorsal cord, we dissected the

cord from the ectodermal tissue, keeping the nerve bundles intact. This revealed many neurites projecting in an anterior-to-posterior direction along the length of the cord, with some neurites projecting laterally (Fig 6E).

FMRFamidergic neurons: We used the rabbit polyclonal anti-FMRFamide to identify potential FMRFamidergic neurons in 3GS stage embryos. This antibody has been shown to be cross-reactive in a diverse set of bilaterians including echinoderms, where reactivity is observed in the radial nerve cord, tube feet, apical muscle, intestine, and the esophagus nerve plexus (Hoekstra et al., 2012). While the exact epitope that is recognized is uncertain, some studies have also found that the FMRFamide antibody exhibits cross-reactivity with SALMFamides and GFSKLYFamide in the sea cucumbers (Ajayi and Withyachumnarnkul, 2013; Diaz-Miranda et al., 1995). Therefore, the possible affinity to other neuropeptides must be considered in *S. kowalevskii.* The labelling shows significant overlap with the *in situ* data for PC2 and GPC, the two enzymes involved in the processing of neuropeptides, so this data provides information about the projection of a subset of neuropeptides within the complement in *S. kowalevskii*.

The peptidergic labelling from this antibody shows a broad circumferential distribution of neurons in the proboscis, but with a concentration at the proboscis base of both cell bodies and axons (Fig 6F). Neurons at the proboscis base have a flask-shaped morphology like the morphology of many other neurons described in this study, with a single cilium extending into the outer ectoderm (Fig 6F). These neurons appear to project posteriorly down the proboscis stem and along the dorsal collar cord, with some projections following the nerve plexus along the collar epithelium (Fig 6F, Fi) connecting with the ventral cord along the trunk (Fig 6F). Cell bodies are detected in the ventral cord with axons running the length of the cord. In the postanal tail of the juvenile, axons are clearly projecting anteriorly (Fig 6Fii). We examined labelling of the adult nervous system by dissection of the ectoderm from the mesoderm in the proboscis and imaged the plexus (Fig 6G). This revealed an extensive plexus throughout the proboscis

ectoderm with a general trend of bundled projections along the AP axis, but with many lateral neurites connecting these bundles projecting both long and short distances.

Neural transgenes

Synapsin transgene: To visualize neurons in higher resolution, we generated a Synapsin construct to drive expression of eGFP. Synapsin is a synaptic vesicle transmembrane protein and a marker of differentiated neurons (De Camilli et al., 1983; Huttner et al., 1983). Our construct was designed using 8 kilobases (KB) upstream of the start site of the synapsin-2-like gene (XP_006820290.1) (Minor et al., 2019). We examined transgene expression in over 50 F_0 juveniles at a range of developmental stages. The transgenic animals exhibit mosaic incorporation of the transgene and show neuronal staining most prominently throughout the proboscis ectoderm, sometimes in the dorsal region of the trunk and collar in isolated neurons (Fig 7A, B). Because of the mosaicism, transgenic animals ranged from a single labeled neuron to hundreds of labeled cells. From these transgenics animals, we identified the range of neural morphologies and the length and directionality of their neural processes. The most common neural morphology we observed with this transgene were large bipolar sensory neurons, like those observed with 5HT immunohistochemistry. We found these neurons throughout the ectoderm, but at highest density in the proboscis. In a separate synapsin:GFP juveniles, we detect large bipolar neurons in the anterior tip of the proboscis projecting posteriorly towards the proboscis base (Fig 7B). At the dorsal proboscis base, neurons have a flask-shape morphology, with a rounded nucleus close to the neural plexus, and with either a single axon, white arrow in inset, or an axon that splits into an anteriorly and posteriorly projecting extension, grey arrow in inset (Fig 7Aii). We also identified a group of elongated sensory neurons in the posterior collar with a single axon projecting anteriorly into the cord, white arrows (Fig 7Aiii). Similar neural morphology was detected in the posterior ectoderm with clear anterior projections (Fig 7Aiv). The projections of this group of neurons are likely involved in relaying posterior sensory

information from the trunk to the anterior part of the animal with most axonal termini at the base of the proboscis. We rarely detected unipolar neurons, but one is shown associated with the plexus projecting anteriorly into the dorsal cord towards the proboscis, grey arrow (Fig 7Aiii). Elongated bipolar neurons are detected in the far posterior ectoderm and project anteriorly along the dorsal midline, likely along the dorsal cord (Fig 7Aiv).

Many of the bipolar neurons have prominent swellings along the axons projecting into the basiepithelial plexus (Fig 7Bi) like what we reported for DiI and serotonin. Many of these varicosities are located close to the basement membrane of the plexus, so it is possible that they may be acting in a paracrine fashion, releasing transmitters/peptides locally, modulating other neurons, directly stimulating muscles through the basement membrane, or representing *en passant* synapses within the plexus. In some cases, we detect what we interpret to be interneurons, closely associated with the neural plexus, co-labelled with DAPI (Fig 7Bii). We also find neurons with a more circular cell body morphology along the mid-proboscis that project anteriorly (Fig 7Biii). In this juvenile, bipolar neurons in the proboscis project posteriorly and appear to terminate at the proboscis base rather than extending further posteriorly (Fig 7B). In other transgenic juveniles, the population of bipolar neurons, right above the first gill slit in the anterior dorsal midline trunk, project anteriorly and terminate at the dorsal proboscis base in many of the animals that were imaged (Fig 7C).

Overall, based on the data from this synapsin transgene, the *S. kowalevskii* ectoderm contains a range of neural cell types including pseudounipolar, bipolar, multipolar, and multiciliated neurons in the proboscis and collar (Fig 7D-G). However, by far the most prevalent type of labeled neuron is the bipolar morphology observed throughout the animal. The abundant bipolar neurons are distinguishable from other types of cells in the ectoderm because of the distinctive axonal projections into the plexus.

Location of transmitter release: eGFP+ neurons from the transgene, DiI staining on fixed tissue, and NeuO labeling in live tissue, all reveal the presence of varicosities along the axons for most of the labelled neurons, most likely the site of transmitter/peptide release, possibly resulting in volumetric transmission or as *en passant* synapses. To further test this and to determine the localization of synapses/transmitter release throughout the nervous system, we designed a construct based on the previous synapsin:eGFP from Figure 7, but with the addition of a mouse synaptophysin-mRuby fusion protein. Synaptophysin is a presynaptic vesicle protein (Pennuto et al., 2003; Wiedenmann and Franke, 1985), so we expect the fusion protein to be transported to either synapses or regions of vesicle release, as has been demonstrated in mouse using a similar construct (Beier et al., 2015). The transgene generates mosaic eGFP expression similar to data presented in Figure 7 (Fig 8A,E). Within these eGFP-labelled neurons, we detect puncta labelled with mRuby, suggesting that the mouse Synaptophysin is trafficked successfully in hemichordates and labels regions of transmitter/peptide release. In the anterior proboscis (Fig 8B), there are many synaptophysin puncta along axons in addition to axon terminus containing a concentration of the synaptophysin fusion protein (Fig 8B,C,D). We observe broad distribution of these puncta in both the anterior (Fig 8B) and posterior proboscis (Fig 8C). Synaptophysin also shows localization around the nucleus and along the cilium in bipolar neurons (Fig 8D). In one striking example, we were able to track a single axon from a cell body in the far posterior to the mid proboscis (Fig 8E). Regular localization of Synaptophysin in swellings along the length of the axon supports our previous suggestion that the neuron is secreting transmitters/peptides locally or making direct neuron-to-neuron connections in the trunk plexus (Fig 8F-H).

Tyrosine hydroxylase transgene: To investigate the cellular morphology and projections of catecholaminargic neurons, we designed a transgene using 5KB of sequence directly upstream of the tyrosine hydroxylase gene. Previously, we established that the cells expressing TH in the proboscis and collar also expressed the dopamine transporter (DAT) supporting the hypothesis that catecholaminergic TH-expressing cells are dopaminergic neurons (Fig 2). The TH:eGFP transgene expression is again

expressed mosaically and mainly restricted to the proboscis, with a few isolated cells in the posterior collar (Fig 9A). Many of the labelled neurons in the proboscis have a flask-shaped morphology, as reported for synapsin:eGFP, and contain a single axonal projection directly into the plexus (Fig 9B,C,F,F'). In about half of the animals imaged, we identified a unique type of cell at the posterior collar and in many cases were able to trace their projections (Fig 9D,E). They have a unique asymmetric cellular morphology; a single dendrite with a terminal sensory cilium, and a protruding vacuole-rich mass. These cells have elaborate axonal trajectories across the collar and often project anteriorly into the proboscis (Fig 9G-I'). Individual neurons were traced and 3D-reconstructed using the 3D Visualization-Assisted Analysis (Vaa3D) software suite. TH transgene-labelled neurons in the anterior proboscis project posteriorly towards the proboscis base (Fig 9F,F') whereas eGFP+ neurons at the proboscis base project anteriorly towards the proboscis tip (Fig 9J-K'). Outside of the proboscis in the few eGFP+ neurons in the collar, neurons project anteriorly towards the proboscis base (Fig 9G-I').

In summary, the transgenic data reveal the detailed cellular morphology of neurons across different regions of the body plan, and for the most part, neurons have a similar morphology; bipolar sensory neurons that project into the neural plexus and often at long distances. Far fewer neurons with detected with more diverse morphologies that were described in classical studies.

Discussion

Distribution of neurons and neural cell types in *S. kowalevskii*

The expression of a wide range of molecular markers of neurons and neural subtypes in *S. kowalevskii* confirms the broad distribution of neurons in the ectoderm outlined in several classical descriptions (Knight-Jones 1952, Bullock, 1940; Bullock, 1945; Hess, 1937). However, unlike the simple neural

plexus proposed by Bullock (1945), our data suggests that the nervous system of enteropneusts is far from simple. The few molecular studies in hemichordate neural structure and organization have focused on the distribution of neurons in the cords, in particular the dorsal cord due to its proposed affinities with the chordate dorsal cord (Nomaksteinsky et al., 2009, Miyamoto and Wada, 2013). Our study provides additional insights, by investigating the entire nervous system including both the cords and the extensive neural plexus. The data clearly identifies a complex arrangement of spatially segregated neural subtypes that is most prominent in the general ectoderm rather than in either cord. The proboscis epithelium is the most richly innervated region of the animal, particularly at the base and close to the proboscis stem on the dorsal side, as has been described in other species of enteropneust (Nomaksteinsky et al., 2009). The collar ectoderm is quite densely populated with neurons but the trunk far less so, but neurons are also concentrated along the midlines in both the dorsal and ventral cords (Fig 1P,S). Data from *elav*, widely used as a pan neural marker, does not seem to label all the neural complement, as some neurons in the epithelium are not *elav*+ as shown by the extensive expression of 5HT in the collar epithelium (Fig 5I).

The strongly regionalized distribution of neural subtype markers in the epithelium of both classical neurotransmitters and peptidergic neurons suggests that there is marked differentiation of the nervous system in both the AP and DV axes (Fig 2,3). At the late juvenile stages, we observed strong regionalization of specific neural markers, densely packed and largely expressed in distinct rings, predominantly in the anterior plexus. However, we also saw evidence of clear molecular differentiation of neural subtypes between the dorsal and ventral cords, but in relatively few markers when compared with expression in the plexus. These data provide a broader view of neural cell type specification throughout the body plan rather than uniquely on cord differentiation (Miyamoto et al., 2010; Miyamoto and Wada, 2013; Nomaksteinsky et al., 2009).

Cell type regionalization in the general ectoderm: We observed the most complex regionalized patterns in the proboscis and collar epithelium, and far fewer in the trunk. However, far from the simple nervous

system proposed by Bullock (1945), our molecular analysis suggests a highly regionalized nervous system with a particularly complex organization at the base of the proboscis: there were three general expression domains; apically restricted, broadly expressed, and localized to the base, with some markers represented in multiple domains. Most of these neural populations show circumferential domains with little evidence of dorsoventral differentiation reflective of the structure of the plexus. The base of the proboscis is both the region of highest neural density and the most diverse in terms of neural cell types. Dopaminergic (DA), GABAergic, histaminergic, and peptidergic neurons show circumferentially localized domains of expression in this region (Fig 2,3), and as we also demonstrate, it is also one of the most distinctive regions of neural plexus organization (Fig 4). The expression of GABA in the proboscis of *P. flava* exhibited a similar distribution to our findings, although their focus was largely restricted to the base of the proboscis and stem (Nomaksteinsky et al., 2009). In the collar, the diversity and density of neurons is less than in the proboscis, and in the trunk of late juveniles, the only 2 neural subtypes represented in the general ectoderm of late juveniles, not associated with the cords, are serotonin and DA.

The rings of neural subtypes in both the collar and proboscis ectoderm are very similar to the expression domains of the regulatory genes with conserved bilaterian roles in CNS patterning described in previous studies on *S. kowalevski* and other enteropneusts species (Kaul-Strehlow et al., 2017; Lowe et al., 2003; Pani et al., 2012). What is particularly striking is the clustering of neural subtypes in the regions of the ectoderm that are the sites of localized epithelial signaling centers during early development. The apical tip of the developing proboscis is the site of active FGF and Hedgehog (Hh) signaling, and a source of Wnt antagonists (Darras et al., 2018; Pani et al., 2012). This territory and has been compared to the vertebrate anterior neural ridge. We observe a wide range of neural subtypes clustered in this region. At early developmental stages, the boundary between the proboscis and collar is the site of a narrow circumferential stripe of transitory Hh expression that strongly resembles the regulatory gene expression profiles of the vertebrate Zona Limitans intrathalamica (ZLI). We notably observed a tight localization of GABA and DA neurons clustered in this region on either side of this organizer. Finally, the boundary of

the collar and trunk is the site of the expression of Wnt1 and FGF8, which are the characteristic ligands of the isthmus organizer at the midbrain hindbrain organizer. This is a key organizer for the formation of the midbrain dopaminergic neurons in vertebrates, and both TH *in situs* and transgenics show TH neurons in this general region. Further functional tests will be required to determine whether these conserved regulatory networks are involved in the regulation of specific neural subtypes in these territories but raises the exciting possibility that conservation of gene regulatory networks between these disparate body plans is related to their role in the positioning of conserved cell types along the AP axis.

Origins of hypothalamus and pituitary: The clustering of neurons around the base of the proboscis that express orthologues of neuropeptides/neurohormones that are involved in the function of the hypothalamic/pituitary axis in vertebrates is of particular interest. Evolutionary insights into the origins of the neurosecretory centers of the vertebrate brain have come from Amphioxus and tunicates, but little is known outside of chordates (Zhang and Ji 2022, Lemaire et al 2021). Studies from the annelid *Platynereis dumerilii* have demonstrated a potential hypothalamic precursor suggesting a deep ancestry of neurosecretory centers in bilaterians (Tessmar-Raible et al., 2007, Denes et al., 2007). Echinoderms and hemichordates have largely been excluded from a broader synthesis, except for the early pioneering studies by Bateson (1885) who compared the proboscis pore at the dorsal base of the proboscis to Hatschek's pit in amphioxus linking it to pituitary and hypothalamic origins, and Komai (1951) who compared the stomocord to the pituitary. The expression of many of the orthologues of characteristic neuropeptides/neurohormones of the hypothalamus (TH, GnRH, CRH, CalC, Orexin) around the base of the proboscis suggest that a more rigorous investigation of this region is warranted to investigate the projections of the neurons expressing neurohormones to determine whether they project to a similar region and whether this territory represents a basic neurosecretory center. Strikingly, the regulatory gene *pitx* (pituitary homeobox) is expressed in a prominent spot at the base of the proboscis (Lowe et al 2006),

and given the regulatory program of both the hypothalamus (Xie and Dorsky 2017) and pituitary is well characterized, this should be investigated in parallel.

Cell type regionalization in the cords: Both the dorsal and ventral cords show characteristic expression domains of specific neural cell types. However, we detect the expression of only a subset of the markers that we see prominently expressed in the proboscis. Despite fewer neural subtypes, those that are expressed show that the cords are distinct molecularly, suggesting differentiation of function. Given our analysis was largely restricted to late juveniles, it is possible that the complement of neural subtypes expands as the animals grow larger. The dorsal cord is divided into the internalized collar cord, and superficial cord than runs the length of the trunk to the anus. We see little evidence of any neurotransmitter marker expression in the collar cord soma, except for peptidergic neurons, despite the prominent expression of *elav*. In the more posterior domains, where the cord is superficial and basiepidermal along the trunk, there are glutamatergic neurons that run down either side of the dorsal cord, and a few isolated GABA labelled cells in the anterior portion of the dorsal cord. Both cords, show clear expression of peptidergic neurons based on the expression of the processing enzymes and several neuropeptides. The length of the ventral cord shows strong and broad expression of the histidine marker HDC.

When the expression of a wide range of markers of neural differentiation are considered, in both the epidermis and in the cords, we see that most neurons at the late juvenile stage are in the proboscis ectoderm rather than in the cords. The region of the highest neural density and diversity is in the proboscis ectoderm, around the base. A previous study in *P. flava* (Nomaksteinsky et al., 2009) had identified the proboscis stem as a region with strong neural differentiation, and we confirm this, but we would include the entire proboscis base in this region of rich neural diversity rather than just the dorsal territory. Many of the gene expression domains in this region are organized in circular rings reminiscent

of the expression of nested transcription factors with key roles in neural cell fate determination in vertebrate brain development.

General organizational features of the plexus and cords: Previous studies have revealed the pervasive plexus present throughout the epidermis, and our data further refines the structural details of the plexus adding significant details (Bullock, 1945; Knight-Jones, 1952; Silèn, 1950; Spengel, 1877, 1903). The plexus is more prominent in the proboscis and with a striking change in organization at the proboscis base, where its organization transitions from parallel nerve bundles running along the AP axis, into a mesh of axonal bundles containing both serotonergic, GABAergic, and peptidergic processes (Fig. 4). A very similar plexus structure has recently been reported in different acoel species (Hulett et al., 2020). In these cases, it is reported that the reticulated neurite bundles wrap around cell clusters. Dilly (1969) reported that the enteropneust epithelium is strongly bound to the basement membrane by cellular processes that penetrate this plexus, so it is possible that this territory has its distinctive morphology due to cells penetrating and attaching to the basement membrane. The plexus is much thicker at the proboscis base and is most prominent on the dorsal side and possibly represents a center of integration (Nomaksteinsky et al., 2009). While this structure is most striking at the base of the proboscis, a looser mesh of axonal bundles is also present in the collar. Confocal z-stacks of the plexus, stained with neural antibodies or following DiI labelling, show that the plexus clearly has some apico/basal structural organization throughout the proboscis and collar suggestive of a partitioning of function – a scenario explicitly rejected in classical studies (Bullock, 1945).

Data from the transgenic embryos give particularly valuable insights into the structure of the plexus, as the mosaic incorporation of the transgene labels only a subset of neurons and enables the tracking of individual neurites. We see no evidence of a plexus organization like that of the simple nets of cnidarians, in which local projections synapse directly to neighboring neurons. Instead, we largely observe long range projections from sensory neurons in the epithelium. Neurons in the anterior proboscis mostly project

posteriorly to the base of the proboscis. However, there is a wide range of axonal trajectories observed, and at the base of the proboscis we observed mostly lateral projections, but also some projections anteriorly. The few cells labelled in the trunk project anteriorly into the proboscis. In some experimental embryos, we were able to trace the neurite from the tip of the tail all the way up to the base of the proboscis, suggesting very long-range communication in the animal (Fig. 6E). We were unable to find a single instance of the axonal projections crossing the basement membrane and into the muscles, from either immunohistochemistry or transgenic data, representing a wide range of neural subtypes. This finding is significant as there has been some disagreement in the classical papers as to whether there is direct innervation of muscles and evidence of axonal processes crossing the basement membrane, summarized most recently by Dilly (1969). Light microscopy reports were decidedly mixed in their assessments with some confirming axonal crossings, but mostly were cautious and reserved in drawing conclusions (Bullock, 1945; Horst, 1939; Knight-Jones, 1952; Silèn, 1950). In Hyman's invertebrate treatise, she concluded there was no compelling evidence for fibers crossing the basement membrane (Hyman, 1955). With the advent of electron microscopy this issue was revisited: two independent studies suggest direct innervation of muscles from fibers crossing the basement membrane (Dilly, 1969; Nørrevang, 1965), but neither study report evidence of neuromuscular junctions. This question would clearly benefit from further clarification using modern serial approaches such as serial block face SEM (Lippens et al., 2019). Comprehensive examination of the sister group to hemichordate, the echinoderms, has shown a similar lack of direct muscular innervation and penetration of the basement membrane by neural fibers in any echinoderm group examined (Cobb and Pentreath, 1977, 1978; Nieuwenhuys, 2000). Even in chordates, Amphioxus, the most basally branching chordate lineages, muscle fibers extend to the neural tube and stimulation occurs at this basement membrane interface (Flood, 1966), suggesting that sophisticated animal behavior can be mediated without a direct neuromuscular junction.

Our data further provides insights into the potential predominant mode of neural transmission in *S. kowalevskii*. The transgene and DiI data are particularly informative: all axons observed at high

magnification were characterized by regular varicosities along their length. One striking synapsin transgenic embryo showed regularly spaced varicosities along the axon of a single neuron from the tail all the way up into the base of the proboscis (Fig 8E-H)). Synaptophysin protein localized to the varicosities suggesting that transmitter/neuropeptide release occurs along the length of the neuron. Varicosities were also pervasive in the proboscis neurons lending support to the idea that, like in echinoderms, communication may largely be paracrine across the plexus, with general transmitter/neuropeptide volumetric release. Volumetric transmission is recognized as a critical component of a wide range of neural systems from the simple to the more complex (Descarries et al., 2008; Descarries et al., 1997; Descarries and Mechawar, 2000; Nicholson, 2000; Nieuwenhuys, 2000). In many extant nervous systems, from vertebrates to *C. elegans* and marine larvae, paracrine, chemically wired brain centers are integrated with synaptic networks, and some authors have proposed that most extant nervous systems likely evolved from peptidergic, paracrine systems (Jekely, 2021). We propose that during the early ambulacrarian evolution paracrine signaling was evolutionarily favored as the predominant mode of neural transmission. We cannot rule out the presence of true synapses between neurons in the plexus and the cords, but at least in the juveniles we examined the presence of neuromuscular junctions is unlikely, and we saw no evidence of the presence of axonal processes crossing the basement membrane into the muscle as was reported by early EM studies (Dilly, 1969). However, it is possible that these develop as the animals grow larger. Nieuwenhuys from his review of volumetric transmission across animal groups (Nieuwenhuys, 2000) makes the key statement that “the notion that volume transmission is primitive, generalized, sluggish and lacks precision, whereas wiring transmission is advanced, specialized, fast and accurate, is erroneous.” Our data needs to be corroborated by neurophysiological assays to determine the function of the nervous system in enteropneusts, but already sets up some clear hypotheses that can be further tested by some targeted serial EM to investigate the detailed structure in the plexus at a variety of regions of the body plan. Of course, this is a description of a single species representing one family of enteropneusts. Follow up studies in additional species, representing a broader range of diversity, will be required to

857 determine whether the details of *S. kowalevskii* neuroanatomy adequately represents the main
858 organizational features of enteropneusts.

859 **Central or decentralized nervous system**

860 Much of the comparative interest in enteropneusts has been in its potential to provide insights into the
861 early origins of chordates. The structure of the nervous system is a critical character for inferring ancestral
862 states of early deuterostome nervous system (Holland et al., 2015). Our data provides some insights into
863 this question, but also raises many others. A simple statement to satisfy whether enteropneusts are
864 characterized by a central nervous system clearly delineated from a peripheral nervous system seems
865 largely driven by our expectations based on studies from highly derived, cephalized model animals. Our
866 data does not provide a clear answer to the question.
867
868 The transgenic animals are the most informative on this issue as they reveal that the predominant neural
869 cell type is a bipolar sensory neuron that project long distances, both in the proboscis and in the trunk. We
870 found scant evidence of the multipolar neurons described in classical studies at the basal side of the
871 plexus. In a few animals, we identified what we interpreted as a potential interneuron close to the
872 predominant bipolar sensory neurons in the tip of the proboscis, and a few instances of multipolar neurons
873 in the proboscis plexus (Fig 7). From our data so far, it is difficult to delineate a distinction between a
874 clearly defined central nervous system and a peripheral nervous system. A previous molecular study
875 (Nomaksteinsky et al., 2009) concluded that the dorsal cord and proboscis stem represented a “bonafide
876 CNS” and the rest of the proboscis and remaining epithelium was a peripheral nervous system. Our data
877 does not support such a strong division, as most neurons identified are sensory, with few candidates for
878 interneurons. At least at this juvenile stage, a division between peripheral and central is not obvious, and
879 the varicosities throughout the plexus are likely involved in processing sensory information. Our data
880 does support an important role of the dorsal proboscis stem as a region of potential integration
881 (Nomaksteinsky et al., 2009), as we observe many of axonal processes from transgenic embryos

882 projecting to this region consistent with previous hypotheses, but the entire proboscis base may be a
883 region of integration rather than simply the dorsal side. We find little support for a special role of the
884 dorsal cord as an integrative center, but perhaps the cords take on more significant roles in processing as
885 the animals grow as our data largely involved studies of late juveniles. However, the characterization of
886 the rest of the proboscis representing a peripheral nervous separated from a central nervous system is not
887 well supported. Our transgene data supports extensive release throughout the plexus and may suggest that
888 information processing occurs throughout the plexus of the animal. The broad dispersal of many neurons,
889 characterized by peptidergic and classical transmitters, particularly in the proboscis and collar, also
890 suggests that signal propagation occurs through tiling in a manner that has been proposed to represent
891 ancestral nervous system function (Jékely 2021), and the characterization of the animal as having a "skin
892 brain" may be the best analogy (Holland, 2003). Whether these varicosities represent true synapses or
893 regions of volumetric release will require more detailed analysis with EM.
894
895 In conclusion, these data further build on existing data from classical studies in demonstrating that
896 hemichordates do not share many organizational principles of the canonical centralized nervous systems
897 of the main models that we study in neurobiology. This study in enteropneusts demonstrates that we have
898 much to discover by sampling a far more diverse array of neural systems representing the rich
899 biodiversity of the marine environment. Our molecular characterization does not reveal cryptic
900 similarities with chordates that were not apparent from previous descriptive work. Yet, despite these
901 profound differences in neural architectures, the early ectodermal patterning that establishes the
902 contrasting neural systems of vertebrates and hemichordates is highly conserved (Lowe et al 2003, Pani et
903 al 2012, Yao et al 2016). This work further develops the counterintuitive observation that regulatory
904 conservation between distantly related groups has seemingly not restricted morphological diversification
905 to a specific neural conformation over macroevolutionary time frames. We are far from understanding the
906 link between gene regulatory conservation and nervous system evolution, and only by broadening our
907 molecular scope into biodiversity are we likely to be able to recognize cryptic links between

908 morphological and molecular evolution that will allow us to address these important but difficult
909 questions of nervous system origins.

910 ## Materials and Methods

911 ### Animal collection and embryo culture

912 Adult worms were collected in the months of May and September during the *S. kowalevskii* breeding
913 seasons in Waquoit Bay, MA., and maintained in flow-through sea tables at the Marine Biological
914 Laboratory in Woods Hole, MA. Spawning fertilization and embryo culture followed protocols developed
915 by Colwin and Colwin (1950, 1962) with updated methods (Lowe et al., 2004).
916

917 ### Cloning of orthologs

918 *S. kowalevskii* homologs of vertebrate genes were identified in an EST library screen (Freeman et al.,
919 2008). See Supplemental Table for NIH accession numbers.
920

921 ### *In situ* hybridization

922 Whole mount *in situ* hybridization on juveniles was carried out using an established lab protocol (Lowe et
923 al., 2004). Embryos were kept in 5mL glass vials for all steps until the colorimetric reaction performed in
924 6 well tissue culture plates. Proteinase K treatment was carried out at 10µg/mL in PBTw for 15min at
925 room temperature (RT). Acetic anhydride treatment at 250µM for 5min at RT followed by a 500µM
926 treatment for 5 min at RT. *In situs* for experimental embryos were stained using 1.6µL:2.7µL ratio of 5-
927 Bromo-4-chloro-3-indolyl phosphate**:** nitro-blue tetrazolium chloride and stopped with 3x5 minute rinses
928 at RT in 1XMAB. Some samples were further cleared by rinsing 2×5 min in MeOH and cleared with a
929 2:1 ratio of benzyl benzoate: benzyl alcohol (BBBA) before imaging on a Zeiss Axioimager.

Whole mount *in situ* hybridizations on adults up to four gill slits utilized the same protocol as embryos with minor modifications: Samples were permeablized for 15-20 minutes at room temperature in Proteinase K diluted 1:7,500 in 1X PBST to increase probe penetration and staining in deeper tissues. The proboscis coelom and gut were punctured with a tungsten needle or scalpel blade to reduce probe trapping and increase penetration. For adult whole mount *in situ* hybridization, samples were dissected using a scalpel or scissors to reduce probe trapping and increase staining of deeper tissues. The whole mount *in situ* hybridization protocol was modified for adults by utilizing either large glass vials or 15 mL tubes and performing at least two more washes than embryos for all steps.

In situ hybridization on tissue sections was based on the protocol for embryos with technical modifications for slides. Fixed adults were dissected into pieces no more than 3 cm in length and cryoprotected in an increasing concentration gradient of sucrose in fixation buffer up to 20% sucrose at room temperature and allowed to equilibrate overnight at 4°C. Samples were then placed in 20% sucrose in fixation buffer diluted 2:1 in OCT media (Fisher) and allowed to equilibrate at room temperature with gentle agitation. Fixation buffer was utilized instead of 1X PBS to reduce tissue swelling and sectioning artifacts. Samples were embedded in plastic molds, chilled on dry ice, and stored indefinitely at -80°C. Frozen blocks were sectioned at 16-25 mm using a Leica cryostat with a cutting temperature between -25 and -30°C. Sections were collected on Superfrost Plus slides (Fisher), allowed to dry for at least 20 minutes, and either processed for *in situ* hybridizations or immunofluorescence immediately or stored at -80°C. Sections were permeablized with 0.2% Triton X-100 in 1X PBST for 20 minutes rather than with Proteinase K, and all washes were performed in upright slide mailers. For hybridization, sections were covered using plastic Hybrislip cover slips (Grace Technologies) and placed facing up in horizontal slide mailers with a Kimwipe or filter paper soaked in hybridization solution to prevent the slide from drying. Slide mailers were sealed using tape, placed in chambers constructed from empty pipette tip boxes, and hybridized overnight in an oven at 60°C. For blocking and antibody steps, sections were outlined using a

hydrophobic marker, and incubations were performed on slides placed horizontally in humidified chambers at room temperature or at 4°C overnight. Different probes were hybridized in separate chambers.

Hybridization Chain Reaction (HCR) in situ hybridization: DNA probe sets were generated and ordered from Molecular Instruments, Inc. using the full RNA sequence from GeneBank accession numbers TH (XM_006813504.1), DAT (NM_001168055), VGLUT (XM_002739644), GAD (XM_002740628), achatin (XM_002732101.2), CCK (XM_002738068.2), and orexin (XM_002734948.2). 11-33 probe sets were generated for each gene, and DNA oligo pools were resuspended to a final concentration of 1μmol/μl in 50 mM Tris buffer, pH 7.5. HCR amplifiers, B1-Alexa Fluor-546, B2-Alexa Fluor-488, and B3-Alexa Fluor-647, were ordered from Molecular Instruments, Inc. HCR version 3.0 protocol (Choi et al., 2018), and a protocol from Nipam Patels lab.

Immunohistochemistry

Juveniles were reared and fixed as previously described (Lowe et al., 2004) Briefly, embryos were fixed for 30 min at room temperature in fixation buffer (3.7% formaldehyde, 0.1 M MOPS pH 7.5, 0.5 M NaCl, 2 mM EGTA pH 8.0, 1 mM MgCl2, 1X PBS), and subsequently stored in ethanol at −20 °C. For anti-GABA, we used 3.7% formaldehyde and 0.3% glutaraldehyde. For antibody staining, embryos were rehydrated into 1x PBS +0.1% Triton X-100 (PBSTr), rinsed 3 × 10 min in PBSTr, and placed into a blocking solution of 1x PBS +0.1% Tween 20 (PBT) +5% goat serum for 2 h at room temperature. Embryos were incubated in PBT with either anti-GFP (Life Technologies, #A-6455), anti-FMRFamide (Immunostar, #20091), anti-5HT (Sigma, S5545), or anti-GABA (Sigma, A2052) at a 1:500 dilution overnight at 4 °C. After primary antibody incubation, embryos were washed 4 × 30 min in PBSTr, and then incubated for 4 h at room temperature with secondary antibody (Alexa-Fluor 488 goat anti-rabbit IgG, ThermoFisher #A-11008) diluted 1:500 in blocking solution. Samples were then washed 4 × 30 min

in PBSTr and cleared into 80% glycerol. Some samples were further cleared by rinsing 2 × 5 min in MeOH and cleared with a 2:1 ratio of benzyl benzoate: benzyl alcohol (BBBA). Images were captured on a ZEIS LSM 700 confocal microscope with 20× and 40× objectives using the Zen software package (Carl Zeiss).

Immunofluorescence on adult tissue sections was performed as described previously with minor modifications. Sections were outlined with a hydrophobic marker, and wash steps were performed in an upright slide mailer. Blocking and antibody incubation steps were performed on slides placed horizontally in humidified chambers at room temperature. Primary antibody incubations were: 1E11, 1:3 (gift of Robert Burke); rabbit anti-serotonin, 1:250 (Sigma S5545); mouse anti-FMRFamide, 1:600 (Immunostar #20091). Secondary antibody (Molecular Probes) dilutions were: Alexa Fluor 488 goat anti-mouse or rabbit, 1:500; Alexa Fluor 546 goat anti-mouse or rabbit, 1:1000; Alexa Fluor goat anti-mouse or rabbit 647, 1:250. Imaging was performed using a Zeiss LSM700 confocal microscope with Zeiss Zen software, an Olympus FV1000 confocal microscope with Olympus software, or a Zeiss Axioimager.Z1 compound microscope or Discovery.V12 stereomicroscope with an Axiocam MRm camera and Zeiss Axiovision software.

Transgenes

5-8kb of putative promoters and enhancers sequence directly upstream of the start codon for genes TH (5kb, XM_006813504.1) and synapsin (8kb, XP_006820290.1) were cloned into a reporter plasmid based designed for developmental studies in Lampreys (Parker et al., 2014) containing I-SceI meganuclease restriction sites, upstream of an eGFP coding sequence and a SV40 late polyadenylation signal sequence using Gibson assembly (Gibson et al., 2009; Parker et al., 2014) and previously published (Minor et al., 2019). Full regulatory sequence for each transgene is included in Supplementary Table 1. Injection mixtures contained 10µl restriction digest including 5 units of I-SceI enzyme (NEB), 1µl CutSmart buffer,

and 130ng of reporter plasmid, final concentration 13ng/µl. The mixture was incubated at 37 °C for 40 min and injected into embryos between 4-9 min post fertilization as previously described (Minor et al., 2019). To visualize regions of transmitter release, the mouse synaptophysin-mRuby fusion protein was cloned into the generated synapsin:eGFP transgene from AAV-FLExloxP-mGFP-2A-synaptophysin-mRuby (Addgene Plasmid# 71760) plasmid vector courtesy of Liqun Luo (Beier et al., 2015) to generate the synapsin:mGFP-2A-(mouse)synaptophysin-mRuby transgene. Vector inset sequence and primers used for the generation of these plasmids are listed in Supplementary Table 1. Reconstruction of neural projections for a subset of neurons were generated using the 3D Visualization-Assisted Analysis (Vaa3D) software suite (Peng et al., 2014).

Acknowledgements

We would like to thank the Staff of the Marine Biological Laboratory for hosting us and their assistance in pursuit of our research. The Waquoit National Estuarine Research Reserve for allowing access to our collection site. Jim Mcilvain from Zeiss for assistance in microscopy, Robb Krumlauf and Hugo Parker for providing the vector for our transgenics. Thurston Lacalli for his guidance and discussions on the evolutionary implications of this work, and Laurent Formery for his editorial input. This work was supported by an NSF grant (1656628) to CJL**.**

Figure Legends

Figure 1: Pan-neural marker, *elav*, expression

(A) An illustration representing the transverse and sagittal sections taken along the adult body. (B, C) Transverse sections at the base of the proboscis show circumferential *elav* expression, with most extensive expression at the far proboscis base. (D-F) Anterior collar sections with dorsal to the right. (E) Higher magnification of the inset from D focused on the proboscis stem. *elav* staining in both the

ectoderm and pharyngeal epithelium (PhEp) and in the anterior collar ring (ACR). (G-I) sections from the posterior collar with I showing a high magnification of inset from (H). (J) Section at the posterior trunk with expression in both dorsal (DNC) and ventral cords (VNC). (K-M) Sagittal sections from proboscis to anterior trunk. (K) Left of the midline, (L) on the midline showing the dorsal cord through the collar, and (M) to the right of the midline. (N, O) Late juvenile stage, whole mount. (N) Lateral view and (O), dorsal view of proboscis and collar. (P) *Elav* expression in dissected adult trunk ventral ectoderm showing the ventral cord. (Q) Whole mount adult proboscis dorsal view. (R) Dorsal view of adult anterior trunk. (S) Dorsal view of posterior trunk. Scale bars equal 250 µm, except in P-S 500 µm.

Figure 2: Expression of neurotransmitter markers

Gene expression in juvenile and adult tissue for components of neurotransmitter synthesis and transport genes. (A-B') *Tyrosine Hydroxylase*. White arrowheads indicate expression at the base of the proboscis, open arrowhead at the tip of the collar, and black arrowhead at the anterior trunk. (A) Expression in early juvenile lateral view, (A') late juvenile lateral view. (B) Whole mount expression in adult proboscis, (B') lateral view of adult collar and base of proboscis. (C-C''') coexpression of tyrosine hydroxylase and dopamine transporter in (C), early juvenile lateral view (AP – anterior proboscis, PB-proboscis base, and AC – anterior collar) with (C') a high magnification of the anterior proboscis, and (C"), a high magnification of the base of the proboscis. (C''') Proboscis and collar of late juvenile. (D) Lateral view of an early juvenile showing expression of *tryptophan hydroxylase*. (E,E') Expression of *histidine decarboxylase* (white arrow indicates base of proboscis) in (E), early juvenile, and (E'), late juvenile. (F-F'') Expression of *vesicular glutamate transporter* in (F), early juvenile, lateral view with lower inset showing dorsal view of the collar and anterior trunk, (F'), dorsal view of later juvenile of the proboscis and collar and (F"), dorsal view of the trunk of a late juvenile. (G-H') Expression of *glutamate decarboxylase* in (G), early juvenile and (G'), late juvenile in lateral view, (H), whole mount of adult tip of the proboscis, (H'), dorsal view of the adult collar and posterior proboscis. (I) Lateral and (I') dorsal

view of *vesicular GABA transporter* expression in early juvenile. Scale bars are 100 µm in early juveniles, 200 µm in late juveniles, and 500 µm in adults.

Figure 3: Expression of neuropeptide markers

Gene expression in early and late juveniles for components of neuropeptide signaling including synthesis and transport genes. (A-C’’’) Co-expression of three neuropeptide synthesis genes in early juveniles in (A) lateral and (B) dorsal views. (C-C’’’) Zoomed-in panels of the dorsal proboscis. (D) *Proprotein convertase 2* expression in early juvenile lateral view, and (D’), expression in late juvenile, both in lateral view. (E) Expression of *glutaminyl-peptide cyclohydrolase* in P, early juvenile, and (E’), late juvenile. (F)Vasotocin expression in early and (F’) late juvenile. (G) Expression of VLamide (VIG) in early and (G’) late juvenile, and with inset showing a dorsal view (G) and lateral view (G’). (H) Expression of Luqin in (H), early juvenile and (H’), late juvenile. (I) Gonadotropin-Releasing Hormone expression in early and late (I’) juvenile. Zoomed-in inset (I) shows proximal axonal projections from neurons in the trunk. (I’) Dorsal view of late juvenile. (J) Expression of neuropeptide WFMRFamide in (J), early juvenile, and (J’), late juvenile. (K) Expression of the neuropeptide NNFamide in (K), early juvenile, and (K’), late juvenile, both in lateral view. (L) Corticotrophin-releasing hormone expression in early and late juvenile (L’), inset shows expression at the heart-kidney complex at the proboscis base. (M) *Orexin* expression in (M), early juvenile and (M’) late juvenile, both lateral views. (N) Calcitonin (CalC) expression in early juvenile, with inset showing proximal axon projections at the proboscis, and late juvenile (N’), with inset showing expression using RNA-based probe. (O)Thyrotropin-releasing hormone (TRH) expression in (O), early juvenile with the dorsal view of the proboscis in the inset, and (O’) late juvenile. (P) *Achatin* expression in (P), early juvenile and (P’) late juvenile, both lateral views, with only the proboscis and collar shown in (P’). (Q) Cholecystokinin expression in early and (Q’) late juvenile, lateral views. (R) Co-expression of the neuropeptides NNFamide, TRH, and WFMRFamide in early and

(R'') late juvenile, with insets (R', R''') showing zoomed-in proboscis base. Scale bars are 100 µm in early juveniles and 200 µm in late juveniles.

Figure 4: Neural plexus organization

Visualization of the neural plexus in fixed and live tissue using an anti-synaptotagmin antibody (A-I), DiI (J-M), and Neo O (N). Juveniles are imaged in whole mount, and adult ectoderm by flat mount following dissection and imaging from the basal surface. (A) Maximum projection of a late juvenile stained for synaptotagmin (1E11), lateral view. (B) high magnification section of adult ectoderm at the base of the proboscis. (C) Illustration showing the performed excision of the posterior proboscis ectoderm from an adult animal. (D-I) Expression of synaptotagmin in dissected adult ectoderm in different regions of the body: (D) dorsal proboscis showing dorsal cord, (E) posterior proboscis base dissected as shown in (C), (F) anterior region of the proboscis base, (G) posterior region of the proboscis base, (H) the anterior collar, and (I) the dorsal trunk. (J-M) Lipophilic dye (DiI) injections into adult fixed tissue reveals dye diffusion across the adult plexus in (J) and (K), and neurite cell morphology in (L) and (M). (N) Live neural marker, NeuO, showing similar puncta along neurites seen in fixed tissue in (L) and (M). Scale bars represent 250 µm in A,D,E,I-K and 25 µm in B,F-H,L-N.

Figure 5: Serotonergic nervous system

Investigation of the serotonergic nervous system in juveniles (A-E) and adults (F-Q) using anti-5HT. (A) Maximum projection of a late juvenile lateral view. (B) High magnification of bipolar neurons with a sensory cilium projecting towards the apical region of the epithelium and a single neurite projecting basally into the neural plexus. (C-E) High magnification images from panels shown in (A): (C) posterior proboscis, (D) collar, and (E) trunk. Images are oriented in an anterior (left)-to-posterior(right) and a

dorsal (up)-to-ventral(down) direction. (F-J) Adult ectoderm in the proboscis; (F) mid proboscis, (G, H) base of the proboscis double labelled with synaptotagmin, and the same specimen as in Fig 3E. (I) collar, and (J) trunk. (K) An illustration showing the sagittal sections carried out in adult tissues: All sections oriented with dorsal at the top of the panel with phalloidin labelled in purple, 5HT in white, and DAPI in blue. (L) proboscis, (M) mid-collar, (N) higher magnification of the dorsal collar cord, (O) anterior trunk, and (P) and (Q) showing the tail. Scale bars represent 500 µm in F,I,J,L,M, O-Q, 200 µm in A,G,N, 20 µm in B-E,H.

Figure 6: GABAergic and FMRFamidergic nervous system

Distribution of GABAergic and peptidergic neurons in juveniles and adults using anti-GABA and anti-FMRFamide polyclonal antibodies. (A-Aiii) distribution of GABA in juveniles. (A) Maximum projection of a late juvenile (Black arrows in A point to the ring of GABA neurons at the anterior collar), and higher magnification of the same individual at 3 different regions: (Ai) anterior proboscis, (Aii) anterior dorsal trunk (arrows indicating the dendrites projecting to the outer epithelium of both the ectoderm and endoderm), and (Aiii) endodermal plexus in the pharyngeal gut of the anterior trunk, with neurites projecting around the gill slits (GS). (B-E) Dissected adult tissue at (B) the proboscis base, (C) collar, (D) gill slits at the trunk, and (E) dissected dorsal collar cord. (F) Maximum projection of a late juvenile labeled with anti-FMRF-amide, panels show the position of the subsequent high magnification images; Fi anterior collar and proboscis stem, (Fii) ventral trunk/ventral cord, and (Fiii) postanal tail. (G) Adult proboscis plexus. Scale bars are 100 µm, except 20 µm in panels Ai-Aiii, and Fi-Fiii.

Figure 7: Neural cell morphology and neurite projection using a synapsin:GFP transgene

(A, B) Maximum projection of two representative synapsin:eGFP animals using 8kb regulatory sequence upstream of the synapsin I gene to drive expression of cytoplasmic eGFP. (Ai-Aiv) and (Bi-Bii) are high magnification panels for each juvenile revealing detailed cellular morphology and neurite projections. (Ai) The anterior proboscis plexus, red arrows point to varicosities along neurites. (Aii) The dorsal cord connecting the proboscis and collar, red arrow points to a single axon and green arrow points to a bifurcated axon from neurons projecting into the cord. (Aiii) Dorsal posterior collar, neurons projecting anteriorly along the dorsal collar cord, with red arrows indicating projecting axons. (Aiv) Postanal tail with detailed cellular morphology of neurons projecting anteriorly. (Bi) Anterior proboscis showing sensory cells projecting into the ectodermal plexus. (Bii) Pair of sensory cells in the apical tuft region that appear to project locally to interneuron in the plexus, indicated by red arrows. (Biii) Mid-proboscis with anteriorly projecting sensory neurons. (C) Projection trajectories from neurons in the dorsal posterior collar, right above the first gill slit, projecting anteriorly towards the dorsal proboscis base. (D-G) Representative neural cell type polarities across different animals. Scale bars in A,B represent 100 µm and 20 µm in Ai-G.

Figure 8: Localization of synaptophysin along axons at varicosities

A, E Synapsin:mGFP—T2A—(mouse)Synaptophysin-mRuby expression from two representative animals using 8kb regulatory sequence upstream of the synapsin I gene to drive expression of mGFP and the mouse synaptophysin-mRuby fusion protein cleaved off by the self-cleaving enzyme sequence, T2A. Mosaic expression of Transgene in 2 representative animals Synaptophysin-mRuby (SYP-mRuby) expression is shown in green channel, synapsin:eGFP (SYN:eGFP) expression in magenta, and nuclear stain with DAPI in blue. (A) Transgene expression in the proboscis neural plexus with higher magnification in (B) anterior proboscis, (C) posterior proboscis base, and (D) dorsal posterior ectoderm. (E) Second animal showing a single neuron expressing the transgene, dorsal view. The cell body is in the tail and projects into the proboscis. (F-H) Higher magnification panels along the length neuron: (F) neural

cell body, (G) mid-axon at the dorsal posterior collar, (H) axon terminal at the mid-proboscis. G', H', and H'' are higher magnification images to show SYP-mRuby puncta along the axon, H' is the axon terminal. Scale bars in A,E are 100 µm and 20µm in B-D, and F-H'.

Figure 9: TH:GFP transgene

(A) Maximum projection of a TH:eGFP representative animal using 5KB regulatory sequence upstream of the TH gene to drive expression of cytoplasmic eGFP. (B-D) Higher magnification images at (B) anterior proboscis, (C) ventral posterior proboscis, and (D) ventral collar. (E) Proboscis ectoderm from a different animal showing detailed cellular morphology of TH+ neurons. (F-K') Manually traced axons from sensory neurons that project posteriorly in the proboscis (F, F'), collar neurons that project anteriorly towards the proboscis (G-I'), and proboscis base neurons that project anteriorly towards the proboscis tip (J-K'). Scale bars in A represent 100 µm, 50 µm in F-K, and 20 µm in B-E and F'-K'.

Supplemental Figure Legends

Supplemental Table:

(A) NIH EST accession numbers for *S. kowalevskii* homologs of vertebrate genes identified in an EST library screen (Freeman et al., 2008). (B) Gene sequence and accession number used to generate the HCR hairpins. (C) Primer sequence used to generate fragments for transgene listen in D. (D) Transgene name and sequence used in this study as well as the gene accession number.

Supplemental Movie 1:

A Z-stack along the trunk of an adult clearly showing the layered nature of the plexus against the synaptotagmin 1 (1E11) antibody.

Supplemental Movie 2:

A Z-stack along the collar and trunk of a 3GS juvenile. The 5HT antibody clearly shows the serotonergic nervous system composed of many sensory neurons at the collar and trunk with a basipethelial neural plexus.

References

Ajayi, A., Withyachumnarnkul, B., 2013. Presence and distribution of FMRFamide-like immunoreactivity in the sea cucumber Holothuria scabra (Jaeger, 1833). Zoomorphology 132, 285-300.
Antzoulatos, E.G., Byrne, J.H., 2004. Learning insights transmitted by glutamate. Trends Neurosci 27, 555-560.
Arendt, D., Nubler-Jung, K., 1994. Inversion of dorsoventral axis? Nature 371, 26.
Arendt, D., Nubler-Jung, K., 1996. Common ground plans in early brain development in mice and flies. Bioessays 18, 255-259.
Aronowicz, J., Lowe, C.J., 2006. Hox gene expression in the hemichordate Saccoglossus kowalevskii and the evolution of deuterostome nervous systems. Integrative and comparative biology 46, 890-901.
Bateson, W., 1885. Later stages in the development of Balanoglossus Kowalevskii with a suggestion as to the affinities of the Enteropneusta. Quarterly Journal of Microscopical Science 25, 81-128.
Bateson, W., 1886. The ancestry of the chordata. Quarterly Journal of Microscopical Science 26, 535-571.
Beier, K.T., Steinberg, E.E., DeLoach, K.E., Xie, S., Miyamichi, K., Schwarz, L., Gao, X.J., Kremer, E.J., Malenka, R.C., Luo, L., 2015. Circuit Architecture of VTA Dopamine Neurons Revealed by Systematic Input-Output Mapping. Cell 162, 622-634.
Bromham, L.D., Degnan, B.M., 1999. Hemichordates and deuterostome evolution: robust molecular phylogenetic support for a hemichordate + echinoderm clade. Evolution & development 1, 166-171.
Brown, F.D., Prendergast, A., Swalla, B.J., 2008. Man is but a worm: chordate origins. Genesis 46, 605-613.
Bullock, T.H., 1940. The functional organisation of the nervous system of the Enteropneusta. Biological Bulletin 79, 91.
Bullock, T.H., 1944. The giant nerve fibre system in Balanoglossids. J. Comp. Neurol. 80, 355.
Bullock, T.H., 1945. The anatomical organization of the nervous system of enteropneusta. Quart. J. Microscrop. Sci. 86, 55-112.
Bullock, T.H., Horridge, G.A., 1965. Structure and function in the nervous systems of invertebrates. W. H. Freeman, San Francisco.
Burbach, J.P., 2011. What are neuropeptides? Methods Mol Biol 789, 1-36.

Busby, W.H., Jr., Quackenbush, G.E., Humm, J., Youngblood, W.W., Kizer, J.S., 1987. An enzyme(s) that converts glutaminyl-peptides into pyroglutamyl-peptides. Presence in pituitary, brain, adrenal medulla, and lymphocytes. J Biol Chem 262, 8532-8536.

Byrne, M., Nakajima, Y., Chee, F.C., Burke, R.D., 2007. Apical organs in echinoderm larvae: insights into larval evolution in the Ambulacraria. Evolution & development 9, 432-445.

Cameron, C.B., Garey, J.R., Swalla, B.J., 2000. Evolution of the chordate body plan: new insights from phylogenetic analyses of deuterostome phyla. Proc Natl Acad Sci U S A 97, 4469-4474.

Cannon, J.T., Kocot, K.M., Waits, D.S., Weese, D.A., Swalla, B.J., Santos, S.R., Halanych, K.M., 2014. Phylogenomic resolution of the hemichordate and echinoderm clade. Curr Biol 24, 2827-2832.

Choi, H.M.T., Schwarzkopf, M., Fornace, M.E., Acharya, A., Artavanis, G., Stegmaier, J., Cunha, A., Pierce, N.A., 2018. Third-generation in situ hybridization chain reaction: multiplexed, quantitative, sensitive, versatile, robust. Development 145.

Cobb, J.L., Pentreath, V.W., 1977. Anatomical studies of simple invertebrate synapses utilizing stage rotation election microscopy and densitometry. Tissue Cell 9, 125-135.

Cobb, J.L., Pentreath, V.W., 1978. Comparison of the morphology of synapses in invertebrate and vertebrate nervous systems: analysis of the significance of the anatomical differences and interpretation of the morphological specializations. Prog Neurobiol 10, 231-252.

Cunningham, D., Casey, E.S., 2014. Spatiotemporal development of the embryonic nervous system of Saccoglossus kowalevskii. Dev Biol 386, 252-263.

Danbolt, N.C., 2001. Glutamate uptake. Prog Neurobiol 65, 1-105.

Darras, S., Fritzenwanker, J.H., Uhlinger, K.R., Farrelly, E., Pani, A.M., Hurley, I.A., Norris, R.P., Osovitz, M., Terasaki, M., Wu, M., Aronowicz, J., Kirschner, M., Gerhart, J.C., Lowe, C.J., 2018. Anteroposterior axis patterning by early canonical Wnt signaling during hemichordate development. PLoS Biol 16, e2003698.

Dawydoff, C., 1948. Classe des Entéropneustes., in: Grassé, P.P. (Ed.), Traité de Zoologie, Paris: Libraries de l'Academie de Médecine, pp. 369-453

De Camilli, P., Harris, S.M., Jr., Huttner, W.B., Greengard, P., 1983. Synapsin I (Protein I), a nerve terminal-specific phosphoprotein. II. Its specific association with synaptic vesicles demonstrated by immunocytochemistry in agarose-embedded synaptosomes. J Cell Biol 96, 1355-1373.

de Castro, F., 1950. Die Normale Histologie des Peripheren Vegetativen Nervensystems: Das Synapsen-Problem Anatomisch-experimentelle UntersuchungAnatomisch-experimentelle Untersuchung. Julius Springer.

De Robertis, E.M., 2008. Evo-devo: variations on ancestral themes. Cell 132, 185-195.

De Robertis, E.M., Sasai, Y., 1996. A common plan for dorsoventral patterning in Bilateria. Nature 380, 37-40.

Denes, A.S., Jekely, G., Steinmetz, P.R., Raible, F., Snyman, H., Prud'homme, B., Ferrier, D.E., Balavoine, G., Arendt, D., 2007. Molecular architecture of annelid nerve cord supports common origin of nervous system centralization in bilateria. Cell 129, 277-288.

Descarries, L., Berube-Carriere, N., Riad, M., Bo, G.D., Mendez, J.A., Trudeau, L.E., 2008. Glutamate in dopamine neurons: synaptic versus diffuse transmission. Brain Res Rev 58, 290-302.

Descarries, L., Gisiger, V., Steriade, M., 1997. Diffuse transmission by acetylcholine in the CNS. Prog Neurobiol 53, 603-625.

Descarries, L., Mechawar, N., 2000. Ultrastructural evidence for diffuse transmission by monoamine and acetylcholine neurons of the central nervous system. Prog Brain Res 125, 27-47.

Diaz-Miranda, L., Blanco, R.E., Garcia-Arraras, J.E., 1995. Localization of the heptapeptide GFSKLYFamide in the sea cucumber Holothuria glaberrima (Echinodermata): a light and electron microscopic study. J Comp Neurol 352, 626-640.

Dilly, P.N., 1969. The nerve fibres in the basement membrane and related structures in Saccoglossus horsti (Enteropneusta). Z Zellforsch Mikrosk Anat 97, 69-83.

Dilly, P.N., Welsch, U., Storch, V., 1970. The structure of the nerve fiber layer and neurocord in the enteropneusts. Z. Zellforsch. Mikrosk. Anat. 103, 129-148.

1259 Elphick, M.R., 2010. NG peptides: a novel family of neurophysin-associated neuropeptides. Gene 458,
1260 20-26.
1261 Elphick, M.R., Mirabeau, O., 2014. The Evolution and Variety of RFamide-Type Neuropeptides: Insights
1262 from Deuterostomian Invertebrates. Front Endocrinol (Lausanne) 5, 93.
1263 Elphick, M.R., Mirabeau, O., Larhammar, D., 2018. Evolution of neuropeptide signalling systems. J Exp
1264 Biol 221.
1265 Er, J.C., Leong, C., Teoh, C.L., Yuan, Q., Merchant, P., Dunn, M., Sulzer, D., Sames, D., Bhinge, A.,
1266 Kim, D., Kim, S.M., Yoon, M.H., Stanton, L.W., Je, S.H., Yun, S.W., Chang, Y.T., 2015. NeuO: a
1267 fluorescent chemical probe for live neuron labeling. Angew Chem Int Ed Engl 54, 2442-2446.
1268 Fischer, W.H., Spiess, J., 1987. Identification of a mammalian glutaminyl cyclase converting glutaminyl
1269 into pyroglutamyl peptides. Proc Natl Acad Sci U S A 84, 3628-3632.
1270 Flood, P.R., 1966. A peculiar mode of muscular innervation in Amphioxus. Light and electron
1271 microscopic studies of the so-called ventral roots. J Comp Neurol 126, 181-217.
1272 Fonnum, F., 1984. Glutamate: a neurotransmitter in mammalian brain. J Neurochem 42, 1-11.
1273 Furlong, R.F., Holland, P.W., 2002. Bayesian phylogenetic analysis supports monophyly of ambulacraria
1274 and of cyclostomes. Zoolog Sci 19, 593-599.
1275 Garstang, W., 1894. Preliminary note on a new theory of the phylogeny of the chordata. Zool. Anzeiger
1276 22, 122-125.
1277 Garstang, W., 1928. The morphology of the Tunicata. Quart J. Miscroscop. Sci. 72, 51-189.
1278 Geoffroy-St. Hilaire, E., 1822. Considérations générales sur les vertebrés. Mem. HIst. Nat. 9, 89-119.
1279 Gerschenfeld, H.M., 1973. Chemical transmission in invertebrate central nervous systems and
1280 neuromuscular junctions. Physiol Rev 53, 1-119.
1281 Gibson, D.G., Young, L., Chuang, R.Y., Venter, J.C., Hutchison, C.A., 3rd, Smith, H.O., 2009.
1282 Enzymatic assembly of DNA molecules up to several hundred kilobases. Nat Methods 6, 343-345.
1283 Gonzalez, P., Uhlinger, K.R., Lowe, C.J., 2017. The Adult Body Plan of Indirect Developing
1284 Hemichordates Develops by Adding a Hox-Patterned Trunk to an Anterior Larval Territory. Curr Biol 27,
1285 87-95.
1286 Greer, J.B., Khuri, S., Fieber, L.A., 2017. Phylogenetic analysis of ionotropic L-glutamate receptor genes
1287 in the Bilateria, with special notes on Aplysia californica. BMC Evol Biol 17, 11.
1288 Hejnol, A., Lowe, C.J., 2015. Embracing the comparative approach: how robust phylogenies and broader
1289 developmental sampling impacts the understanding of nervous system evolution. Philos Trans R Soc
1290 Lond B Biol Sci 370.
1291 Hess, W.N., 1937. The nervous system of Dolichoglossus kowalevskyi. Journal of Experimental Zoology
1292 79, 1-11.
1293 Hewes, R.S., Taghert, P.H., 2001. Neuropeptides and neuropeptide receptors in the Drosophila
1294 melanogaster genome. Genome Res 11, 1126-1142.
1295 Hirth, F., 2010. On the origin and evolution of the tripartite brain. Brain Behav Evol 76, 3-10.
1296 Hirth, F., Reichert, H., 1999. Conserved genetic programs in insect and mammalian brain development.
1297 Bioessays 21, 677-684.
1298 Hoekstra, L.A., Moroz, L.L., Heyland, A., 2012. Novel insights into the echinoderm nervous system from
1299 histaminergic and FMRFaminergic-like cells in the sea cucumber Leptosynapta clarki. PLoS One 7,
1300 e44220.
1301 Holland, L.Z., 2015. Evolution of basal deuterostome nervous systems. J Exp Biol 218, 637-645.
1302 Holland, N.D., 2003. Early central nervous system evolution: an era of skin brains? Nat Rev Neurosci 4,
1303 617-627.
1304 Holland, N.D., Holland, L.Z., Holland, P.W., 2015. Scenarios for the making of vertebrates. Nature 520,
1305 450-455.
1306 Horst, C.J.v.d., 1939. Hemichordata. Akademische Verlagsgesellschaft m.b.H., Leipzig.
1307 Hulett, R.E., Potter, D., Srivastava, M., 2020. Neural architecture and regeneration in the acoel Hofstenia
1308 miamia. Proceedings. Biological sciences / The Royal Society 287, 20201198.

Huttner, W.B., Schiebler, W., Greengard, P., De Camilli, P., 1983. Synapsin I (protein I), a nerve terminal-specific phosphoprotein. III. Its association with synaptic vesicles studied in a highly purified synaptic vesicle preparation. J Cell Biol 96, 1374-1388.
Hyman, L.H., 1955. The invertebrates, 1st ed. McGraw-Hill, New York,.
Jackson, F.R., Newby, L.M., Kulkarni, S.J., 1990. Drosophila GABAergic systems: sequence and expression of glutamic acid decarboxylase. J Neurochem 54, 1068-1078.
Jekely, G., 2013. Global view of the evolution and diversity of metazoan neuropeptide signaling. Proc Natl Acad Sci U S A 110, 8702-8707.
Jekely, G., 2021. The chemical brain hypothesis for the origin of nervous systems. Philos Trans R Soc Lond B Biol Sci 376, 20190761.
Kaul, S., Stach, T., 2010. Ontogeny of the collar cord: neurulation in the hemichordate Saccoglossus kowalevskii. J Morphol 271, 1240-1259.
Kaul-Strehlow, S., Röttinger, E., 2015. Hemichordata, in: Wanninger, A. (Ed.), Evolutionary Developmental Biology of Invertebrates 6: Deuterostomia. Springer Vienna, Vienna, pp. 59-89.
Kaul-Strehlow, S., Stach, T., 2013. A detailed description of the development of the hemichordate Saccoglossus kowalevskii using SEM, TEM, Histology and 3D-reconstructions. Frontiers in Zoology 10, 1-31.
Kaul-Strehlow, S., Urata, M., Minokawa, T., Stach, T., Wanninger, A., 2015. Neurogenesis in directly and indirectly developing enteropneusts: of nets and cords. Org Divers Evol 15, 405-422.
Kaul-Strehlow, S., Urata, M., Praher, D., Wanninger, A., 2017. Neuronal patterning of the tubular collar cord is highly conserved among enteropneusts but dissimilar to the chordate neural tube. Sci Rep 7, 7003.
Kinjo, A., Koito, T., Kawaguchi, S., Inoue, K., 2013. Evolutionary history of the GABA transporter (GAT) group revealed by marine invertebrate GAT-1. PLoS One 8, e82410.
Knight-Jones, E., 1952. On the nervous system of Saccoglossus cambriensis (Enteropneusta). . Philos. Trans. R. Soc. Lond. B. Biol. Sci. 236, 315-354.
Komai T. The homology of the" notochord" found in pterobranchs and enteropneusts. The American Naturalist. 1951 Jul 1;85(823):270-1.
Kowalevsky, A., 1866. Anatomie des Balanoglossus. Mem Acad Imp Sci St Petersburg 7, 16.
Krishnan, A., Almen, M.S., Fredriksson, R., Schioth, H.B., 2013. Remarkable similarities between the hemichordate (Saccoglossus kowalevskii) and vertebrate GPCR repertoire. Gene 526, 122-133.
Lemaire LA, Cao C, Yoon PH, Long J, Levine M. The hypothalamus predates the origin of vertebrates. Science Advances. 2021 Apr 28;7(18):eabf7452.
Lichtneckert, R., Reichert, H., 2005. Insights into the urbilaterian brain: conserved genetic patterning mechanisms in insect and vertebrate brain development. Heredity (Edinb) 94, 465-477.
Lippens, S., Kremer, A., Borghgraef, P., Guerin, C.J., 2019. Serial block face-scanning electron microscopy for volume electron microscopy. Methods Cell Biol 152, 69-85.
Lowe, C.J., 2021. Molecular insights into deuterostome evolution from hemichordate developmental biology. Curr Top Dev Biol 141, 75-117.
Lowe, C.J., Tagawa, K., Humphreys, T., Kirschner, M., Gerhart, J., 2004. Hemichordate embryos: procurement, culture, and basic methods. Methods Cell Biol 74, 171-194.
Lowe, C.J., Terasaki, M., Wu, M., Freeman, R.M., Jr., Runft, L., Kwan, K., Haigo, S., Aronowicz, J., Lander, E., Gruber, C., Smith, M., Kirschner, M., Gerhart, J., 2006. Dorsoventral patterning in hemichordates: insights into early chordate evolution. PLoS Biol 4, e291.
Lowe, C.J., Wu, M., Salic, A., Evans, L., Lander, E., Stange-Thomann, N., Gruber, C.E., Gerhart, J., Kirschner, M., 2003. Anteroposterior patterning in hemichordates and the origins of the chordate nervous system. Cell 113, 853-865.
Luo, L., 2020. Principles of neurobiology, Second edition. ed. Garland Science, Boca Raton.
Luttrell, S., Konikoff, C., Byrne, A., Bengtsson, B., Swalla, B.J., 2012. Ptychoderid hemichordate neurulation without a notochord. Integrative and comparative biology 52, 829-834.
Martin-Duran, J.M., Pang, K., Borve, A., Le, H.S., Furu, A., Cannon, J.T., Jondelius, U., Hejnol, A., 2018. Convergent evolution of bilaterian nerve cords. Nature 553, 45-50.

McIntire, S.L., Jorgensen, E., Kaplan, J., Horvitz, H.R., 1993. The GABAergic nervous system of Caenorhabditis elegans. Nature 364, 337-341.
Metschnikoff, V.E., 1881. Über die systematische Stellung von Balanoglossus. Zool Anz 4, 139-157.
Miller, M.W., 2019. GABA as a Neurotransmitter in Gastropod Molluscs. Biol Bull 236, 144-156.
Minor, P.J., Clarke, D.N., Andrade Lopez, J.M., Fritzenwanker, J.H., Gray, J., Lowe, C.J., 2019. I-SceI Meganuclease-mediated transgenesis in the acorn worm, Saccoglossus kowalevskii. Dev Biol 445, 8-15.
Mirabeau, O., Joly, J.S., 2013. Molecular evolution of peptidergic signaling systems in bilaterians. Proc Natl Acad Sci U S A 110, E2028-2037.
Miyamoto, N., Nakajima, Y., Wada, H., Saito, Y., 2010. Development of the nervous system in the acorn worm Balanoglossus simodensis: insights into nervous system evolution. Evolution & development 12, 416-424.
Miyamoto, N., Wada, H., 2013. Hemichordate neurulation and the origin of the neural tube. Nature communications 4, 2713.
Morgan, T., 1894. Development of Balanoglossus. Journal of Morphology 9, 1-86.
Mueller, T., Vernier, P., Wullimann, M.F., 2006. A phylotypic stage in vertebrate brain development: GABA cell patterns in zebrafish compared with mouse. J Comp Neurol 494, 620-634.
Nakajima, Y., Humphreys, T., Kaneko, H., Tagawa, K., 2004a. Development and neural organization of the tornaria larva of the Hawaiian hemichordate, Ptychodera flava. Zoolog Sci 21, 69-78.
Nakajima, Y., Kaneko, H., Murray, G., Burke, R.D., 2004b. Divergent patterns of neural development in larval echinoids and asteroids. Evolution & development 6, 95-104.
Nicholson, C., 2000. Volume transmission in the year 2000. Prog Brain Res 125, 437-446.
Nieuwenhuys, R., 2000. Comparative aspects of volume transmission, with sidelight on other forms of intercellular communication. Prog Brain Res 125, 49-126.
Nistri, A., Constanti, A., 1979. Pharmacological characterization of different types of GABA and glutamate receptors in vertebrates and invertebrates. Prog Neurobiol 13, 117-235.
Nomaksteinsky, M., Rottinger, E., Dufour, H.D., Chettouh, Z., Lowe, C.J., Martindale, M.Q., Brunet, J.F., 2009. Centralization of the deuterostome nervous system predates chordates. Curr Biol 19, 1264-1269.
Nørrevang, A., 1965. Fine structure of nervous layer, basement membrane, and muscles of the proboscis in Harrimania kupfferi (Enteropneusta). Vidensk. Medd. fra Dansk naturh. Foren. 128, 325-337.
Pani, A.M., Mullarkey, E.E., Aronowicz, J., Assimacopoulos, S., Grove, E.A., Lowe, C.J., 2012. Ancient deuterostome origins of vertebrate brain signalling centres. Nature 483, 289-294.
Parker, H.J., Bronner, M.E., Krumlauf, R., 2014. A Hox regulatory network of hindbrain segmentation is conserved to the base of vertebrates. Nature 514, 490-493.
Pennuto, M., Bonanomi, D., Benfenati, F., Valtorta, F., 2003. Synaptophysin I controls the targeting of VAMP2/synaptobrevin II to synaptic vesicles. Mol Biol Cell 14, 4909-4919.
Pham, K., Hobert, O., 2019. Unlike Drosophila elav, the C. elegans elav orthologue exc-7 is not panneuronally expressed. MicroPubl Biol 2019.
Roberts, E., Chase, T.N., Tower, D.B., City of Hope National Medical Center (U.S.), National Institute of Neurological and Communicative Disorders and Stroke., Kroc Foundation., 1976. GABA in nervous system function. Raven Press, New York.
Roberts, E., Kuriyama, K., 1968. Biochemical-physiological correlations in studies of the gamma-aminobutyric acid system. Brain Res 8, 1-35.
Robinow, S., Campos, A.R., Yao, K.M., White, K., 1988. The elav gene product of Drosophila, required in neurons, has three RNP consensus motifs. Science 242, 1570-1572.
Robinow, S., White, K., 1988. The locus elav of Drosophila melanogaster is expressed in neurons at all developmental stages. Dev Biol 126, 294-303.
Rouille, Y., Duguay, S.J., Lund, K., Furuta, M., Gong, Q., Lipkind, G., Oliva, A.A., Jr., Chan, S.J., Steiner, D.F., 1995. Proteolytic processing mechanisms in the biosynthesis of neuroendocrine peptides: the subtilisin-like proprotein convertases. Front Neuroendocrinol 16, 322-361.

Sanfilippo, P., Smibert, P., Duan, H., Lai, E.C., 2016. Neural specificity of the RNA-binding protein Elav is achieved by post-transcriptional repression in non-neural tissues. Development 143, 4474-4485.
Sato, A., Bishop, J.D., Holland, P.W., 2008. Developmental biology of pterobranch hemichordates: history and perspectives. Genesis 46, 587-591.
Seidah, N.G., Benjannet, S., Hamelin, J., Mamarbachi, A.M., Basak, A., Marcinkiewicz, J., Mbikay, M., Chretien, M., Marcinkiewicz, M., 1999. The subtilisin/kexin family of precursor convertases. Emphasis on PC1, PC2/7B2, POMC and the novel enzyme SKI-1. Ann N Y Acad Sci 885, 57-74.
Silèn, L., 1950. On the nervous system of Glossibalanus marginatus Meek (Enteropneusta). . Acta Zoologica 31, 149-175
Spengel, J.W., 1877. Ueber den Bau und die Entwickelung des Balanoglossus. Amtl. Ber. 50,vers.d. Naturf. U. Artz, 176-177.
Spengel JW. Neue Betrage zur Kenntniss der Enteropneusten 1. Ptychodera flava. Zool. Jahrb., Abt. f. Anat., Bd. 1903;18:271-326.
Tassia, M.G., Cannon, J.T., Konikoff, C.E., Shenkar, N., Halanych, K.M., Swalla, B.J., 2016. The Global Diversity of Hemichordata. PLoS One 11, e0162564.
Tessmar-Raible, K., Raible, F., Christodoulou, F., Guy, K., Rembold, M., Hausen, H., Arendt, D., 2007. Conserved sensory-neurosecretory cell types in annelid and fish forebrain: insights into hypothalamus evolution. Cell 129, 1389-1400.
Tinoco, A.B., Barreiro-Iglesias, A., Yanez Guerra, L.A., Delroisse, J., Zhang, Y., Gunner, E.F., Zampronio, C.G., Jones, A.M., Egertova, M., Elphick, M.R., 2021. Ancient role of sulfakinin/cholecystokinin-type signalling in inhibitory regulation of feeding processes revealed in an echinoderm. Elife 10.
van den Pol, A.N., 2012. Neuropeptide transmission in brain circuits. Neuron 76, 98-115.
Walker, R.J., Papaioannou, S., Holden-Dye, L., 2009. A review of FMRFamide- and RFamide-like peptides in metazoa. Invert Neurosci 9, 111-153.
Watanabe, T., Taguchi, Y., Shiosaka, S., Tanaka, J., Kubota, H., Terano, Y., Tohyama, M., Wada, H., 1984. Distribution of the histaminergic neuron system in the central nervous system of rats; a fluorescent immunohistochemical analysis with histidine decarboxylase as a marker. Brain Res 295, 13-25.
Wiedenmann, B., Franke, W.W., 1985. Identification and localization of synaptophysin, an integral membrane glycoprotein of Mr 38,000 characteristic of presynaptic vesicles. Cell 41, 1017-1028.
Xie Y, Dorsky RI. Development of the hypothalamus: conservation, modification and innovation. Development. 2017 May 1;144(9):1588-99.
Yao, Y., Minor, P.J., Zhao, Y.T., Jeong, Y., Pani, A.M., King, A.N., Symmons, O., Gan, L., Cardoso, W.V., Spitz, F., Lowe, C.J., Epstein, D.J., 2016. Cis-regulatory architecture of a brain signaling center predates the origin of chordates. Nat Genet 48, 575-580.
Zhang S, Ji X. Hatschek's pit and origin of pituitary gland. Acta Oceanologica Sinica. 2022 Dec;41(12):1-6.
Zhang, X., Pan, H., Peng, B., Steiner, D.F., Pintar, J.E., Fricker, L.D., 2010. Neuropeptidomic analysis establishes a major role for prohormone convertase-2 in neuropeptide biosynthesis. J Neurochem 112, 1168-1179.
Zoeller RT, Tan SW, Tyl RW. General background on the hypothalamic-pituitary-thyroid (HPT) axis. Critical reviews in toxicology. 2007 Jan 1;37(1-2):11-53.

Figure 1: Pan-neural marker, ELAV, expression

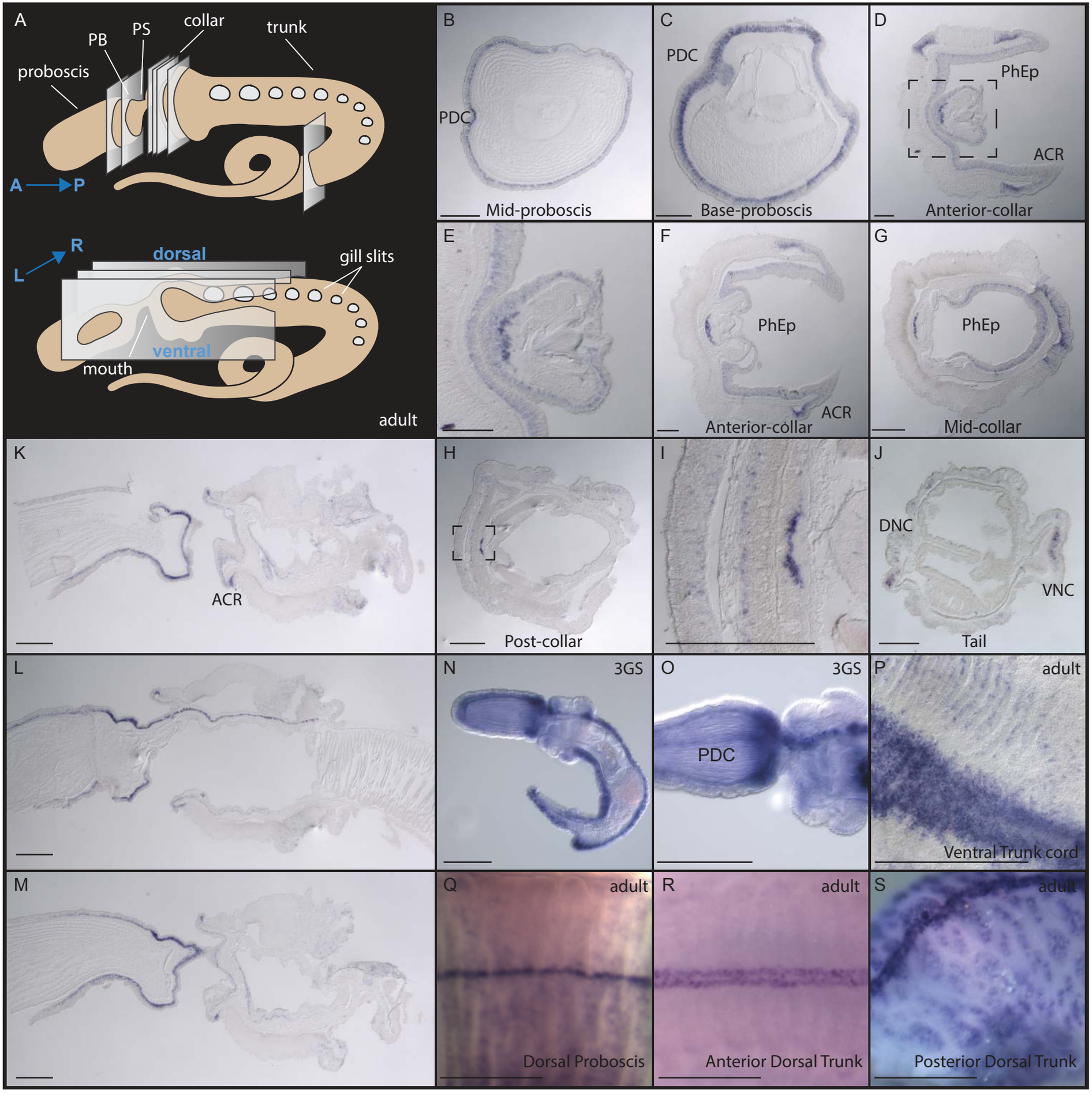

Figure 2: Expression of neurotransmitter markers

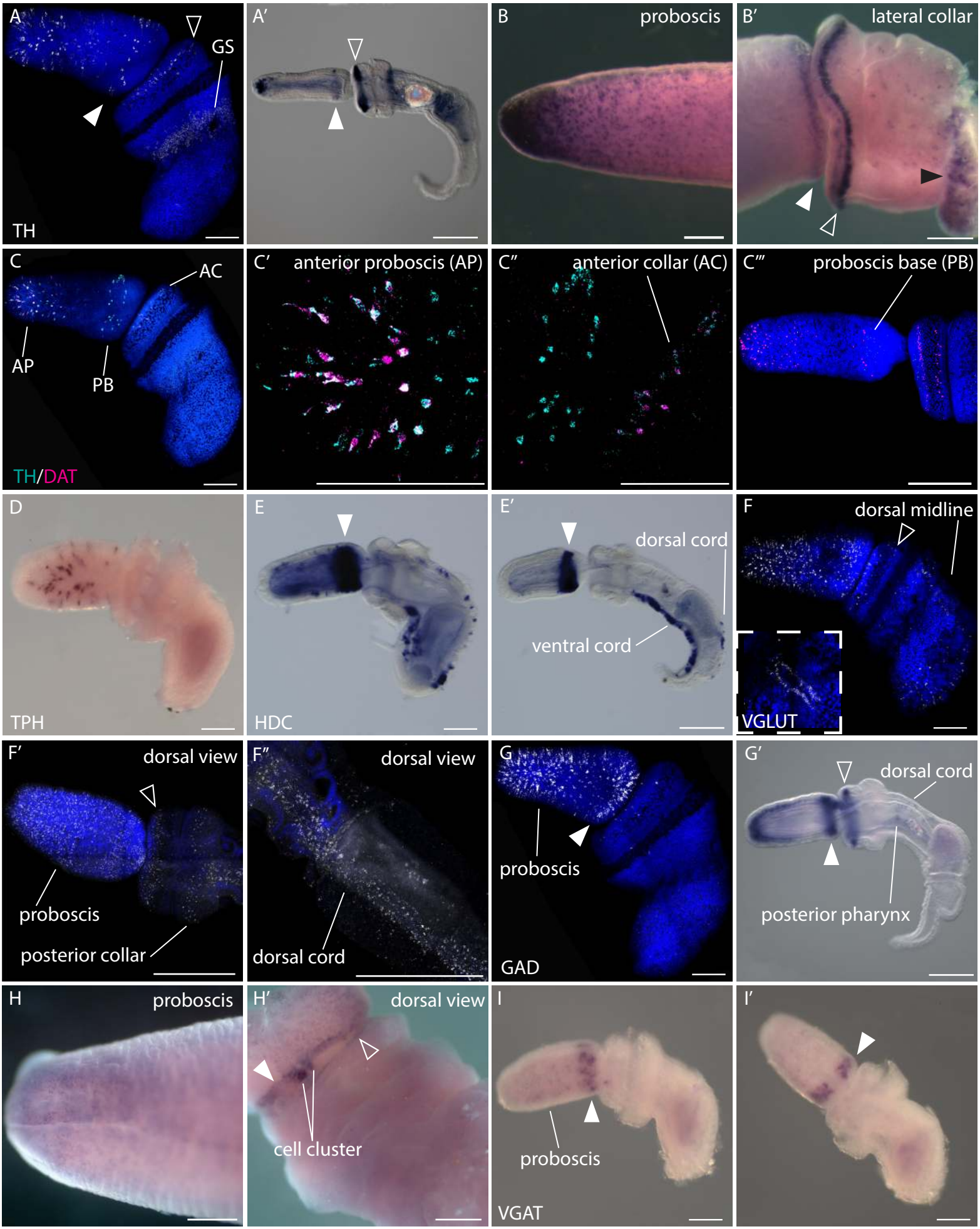

Figure 3: Expression of neuropeptide markers

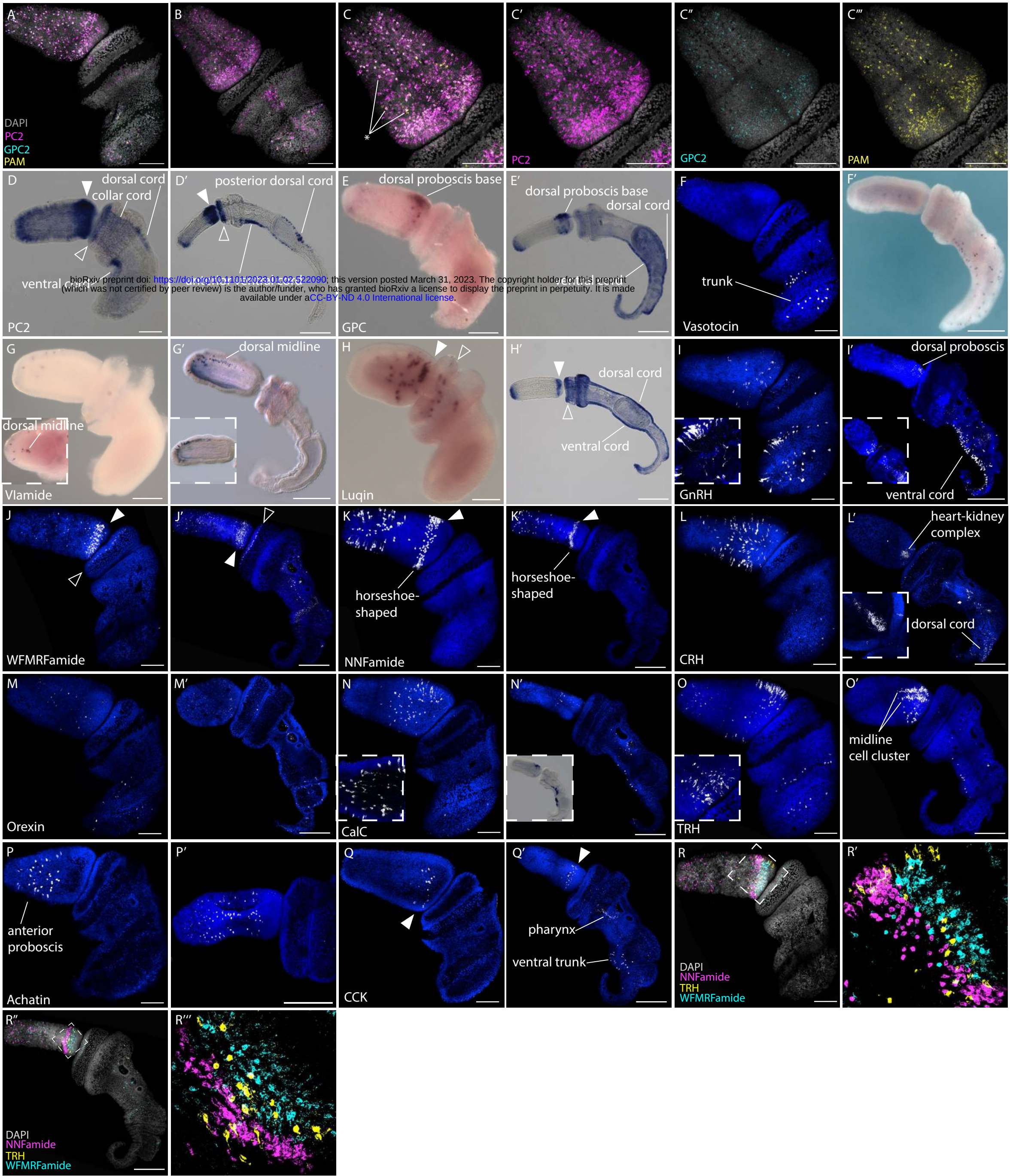

Figure 4: Neural plexus organization

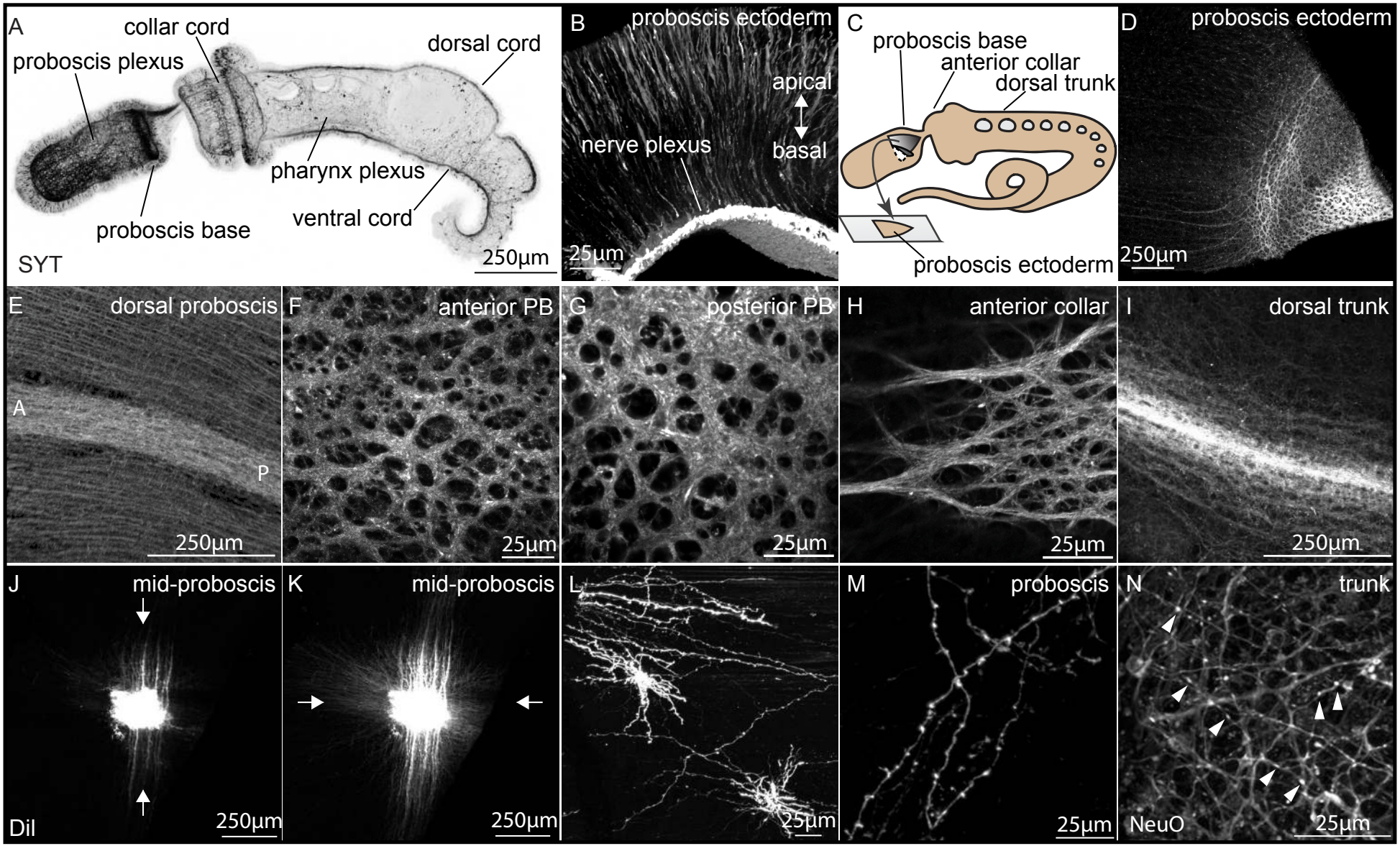

Figure 5: Serotonergic nervous system

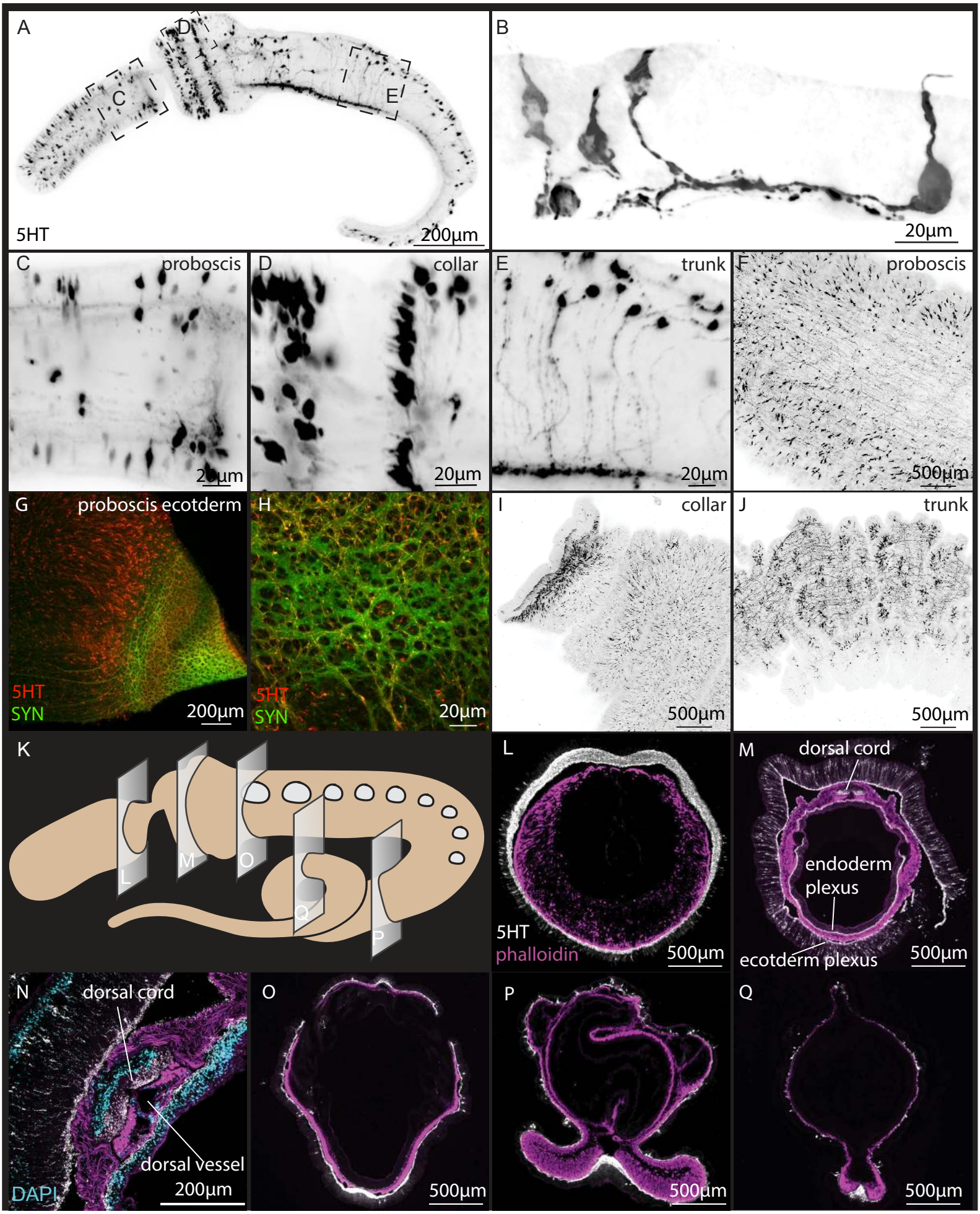

Figure 6: GABAergic and FMRFamidergic nervous system

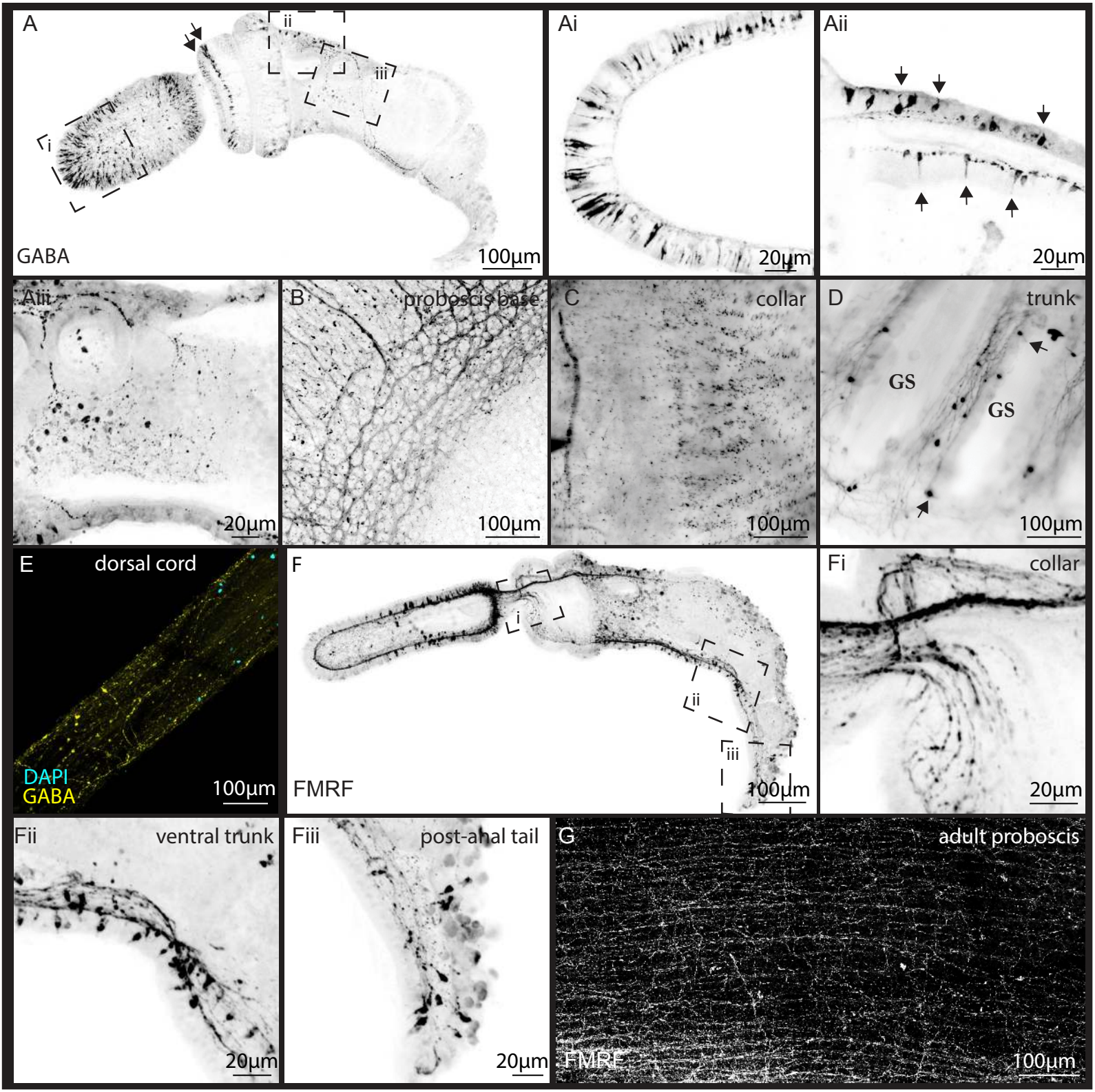

Figure 7: Neural cell morphology and neurite projection using a synapsin:GFP transgene

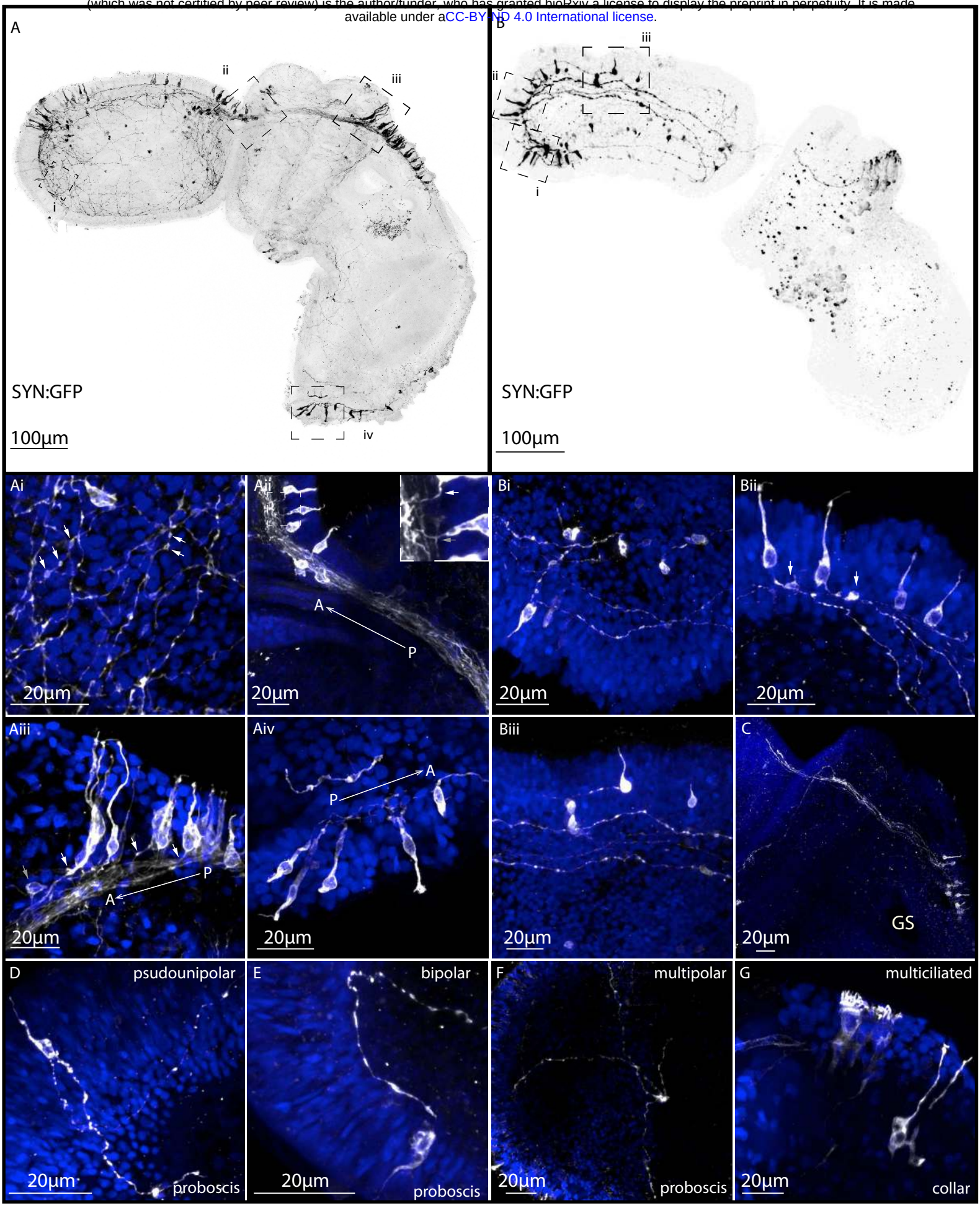

Figure 8: Localization of synaptophysin along axons at varicosities

Figure 9: TH:GFP transgene